Remote Sensing of Environment 171 (2015) 311–325

Contents lists available at ScienceDirect

Remote Sensing of Environment

journal homepage: www.elsevier.com/locate/rse

Effects of fire severity and post-fire climate on short-term vegetation recovery of mixed-conifer and red fir forests in the Sierra Nevada Mountains of California

Ran Meng [a,*,1], Philip E. Dennison [a], Chengquan Huang [b], Max A. Moritz [c], Carla D'Antonio [d]

[a] Department of Geography, University of Utah, 260 s Central Campus Dr., RM 270, Salt Lake City, UT 84112, USA
[b] Department of Geographical Sciences, University of Maryland, 1165 Lefrak Hall, College Park, MD 20742, USA
[c] Department of Environmental Science, Policy, and Management, University of California, 137 Mulford Hall, Berkeley, CA 94720, USA
[d] Department of Ecology, Evolution and Marine Biology, University of California, 4017L Bren Hall, Santa Barbara, CA 93106, USA

ARTICLE INFO

Article history:
Received 5 April 2015
Received in revised form 10 October 2015
Accepted 23 October 2015
Available online xxxx

Keywords:
Fire ecology
Landsat time series data
Sierra Nevada
Post-fire climate
Vegetation Change Tracker (VCT)

ABSTRACT

Forest ecosystems in the Sierra Nevada Mountains of California are greatly influenced by wildfire as a natural disturbance, and increased fire severity and drought occurrence may alter the course of post-fire recovery in these ecosystems. We examined effects of fire severity, post-fire climate, and topographic factors on short-term (<5 years) vegetation recovery in mixed-conifer and red fir forests in the Sierra Nevada. We hypothesized that short-term vegetation recovery patterns would be different among patches with varying fire severity, especially between low-moderate and high severity patches, and that post-fire climate would have differing impacts on short-term vegetation recovery in different ecological zones (lower montane forest vs. upper montane forest). 30-meter Landsat time series stacks were used to monitor short-term vegetation recovery following wildfire in mixed-conifer and red fir forest types. Changes in normalized difference vegetation index (NDVI) following thirty-five fires (>405 ha) between 1999 and 2006 were examined. According to the modeling results provided by ordinary least squares (OLS) regressions including spatial variation coefficients, fire severity, post-fire wet eason precipitation, post-fire January minimum temperature, and topographic factors explain variations in short-term post-fire NDVI values (adjusted R-squared = [0.680, 0.688] for red fir forests; adjusted R-squared = [0.671, 0.678] for mixed-conifer forests). The modeling results indicated that burned mixed-conifer forest was sensitive to post-fire drought, while burned red fir forest, with higher summer soil moisture availability, was sensitive to post-fire temperature. We also found that differences in recovery related to fire severity disappeared more quickly in burned mixed-conifer forest than in burned red fir forest. Future efforts should focus on long-term recovery, including competition between forest and shrub species in previously burned areas.

© 2015 Elsevier Inc. All rights reserved.

1. Introduction

Wildfire has a key role in shaping patterns and processes in terrestrial ecosystems of the western US (Sugihara, Wagtendonk, Fites-Kaufman, & Andrea, 2006). Fire-prone environments have promoted the adaptation of vegetation species in many western US forests, enabling these fire-adapted species to recover following fire (Sugihara et al., 2006). Nevertheless, post-fire vegetation recovery is still determined by many onsite factors, such as fire severity, different plant regeneration strategies, topography, and local climate (Chappell & Agee, 1996; Collins & Roller, 2013; Crotteau, Morgan Varner III, & Ritchie, 2013; Goforth & Minnich, 2008; Russell, McBride, & Rowntree, 1998; Scholl & Taylor, 2006; Shatford, Hibbs, & Puettmann, 2007; Taylor & Halpern, 1991; Taylor & Skinner, 1998).

Previous work has shown strong effects of fire severity on post-fire vegetation recovery (Chappell & Agee, 1996; Crotteau et al., 2013; Donato et al., 2009) and addressed the important role of landscape position and topography in explaining variations in forest establishment following fire over space and time Collins & Roller, 2013; Shatford et al., 2007. In the southern Cascades mountain range (which shares similarities in climate and vegetation with the Sierra Nevada range), Crotteau et al. (2013) found the highest conifer seedling density in medium fire severity patches, with lower density in high severity patches and intermediate density in low severity patches. However, shrub seedling density increased sharply with fire severity (Crotteau et al., 2013). Similar post-fire patterns of seedling establishment were also found in

* Corresponding author.
E-mail address: ranmeng@bnl.gov (R. Meng).
[1] Present address: Environmental and Climate Sciences Department, Brookhaven National Laboratory, Bldg. 490A, Upton, NY 11973, USA.

http://dx.doi.org/10.1016/j.rse.2015.10.024
0034-4257/© 2015 Elsevier Inc. All rights reserved.

high-elevation forests dominated by red fir in the southern Cascades (Chappell & Agee, 1996).

Post-fire climate might also control forest regeneration and interact with factors such as landscape position to alter post-fire recovery (Chappell & Agee, 1996; Collins & Roller, 2013; Goforth & Minnich, 2008; Russell et al., 1998). Chappell and Agee (1996) found that post-fire red fir seedling establishment was higher in mesic areas and that seasonal drought was an important agent of seedling mortality. Elevation, as a proxy for climate, was found to have a strongly negative correlation with seedling density of mixed-conifer forests in the Sierra Nevada (Mantgem, Stephenson, & Keeley, 2006). Seedling dynamics might be the earliest signal of changing forest conditions and can indicate environmental changes (Mantgem et al., 2006). As a result, post-fire climate in the first growing seasons following fire may be highly important for forest regeneration (Donato et al., 2009).

Previous studies have made substantial contributions to our understanding of vegetation recovery following fire in the Sierra Nevada and southern Cascades, but most of them are ground-based and face logistical limitations in the extent of the areas that could be sampled (Chappell & Agee, 1996; Collins & Roller, 2013; Crotteau et al., 2013; Shatford et al., 2007). In contrast, remote sensing-based post-fire studies can provide insights into controls over vegetation responses to wildfire beyond what can be measured in spatially limited ground surveys (Chen et al., 2011; Chu & Guo, 2013; Díaz-Delgado & Pons, 2001; Gitas, Mitri, Veraverbeke, & Polychronaki, 2012; Lentile et al., 2006; Mitri & Gitas, 2013; White, Ryan, Key, & Running, 1996). Fire can affect the spectral and spatial properties of forests by vegetation removal, soil exposure, and soil color alteration (White et al., 1996). Spectral vegetation indices have been extensively examined to quantify post-fire vegetation recovery (Díaz-Delgado, Lloret, & Pons, 2003; Gitas et al., 2012; Ireland & Petropoulos, 2015; Lentile et al., 2006; Riaño et al., 2002; Veraverbeke et al., 2012; Viedma, Meliá, Segarra, & García-Haro, 1997; White et al., 1996). Imaging spectroscopy, lidar, and synthetic aperture radar data have more recently been incorporated into investigations of post-fire vegetation recovery (Huesca et al., 2013; Kane et al., 2013, 2014; Kane, Lutz et al., 2015a; Tanase, Santoro, de La Riva, Pérez-Cabello, & Le Toan, 2010a; Tanase, Santoro, Wegmüller, de la Riva, & Pérez-Cabello, 2010b; Tanase, de la Riva, Santoro, Pérez-Cabello, & Kasischke, 2011), but have limited spatial and temporal coverage.

Land managers endeavor to identify vulnerable areas with poor post-fire recovery potential, and then restore natural forest conditions with priority intervention (Collins, Kelly, Van Wagtendonk, & Stephens, 2007; Collins et al., 2009; Huesca et al., 2013). Thorough and accurate monitoring, evaluation, and understanding of post-fire forest regeneration are essential for assessing effects of disturbances on ecological processes, modeling vulnerability of forest ecosystems, and studying climate-fire regime interactions (Mitri & Gitas, 2013; Solans Vila & Barbosa, 2010). Using forest gap and climate models, optical remote sensing, and lidar data, a number of studies have recently explored the effects of local climate patterns and topography on fire regime and forest structure in the Sierra Nevada in depth (Kane et al., 2013, 2014; Kane, Cansler et al., 2015b; Miller & Urban, 1999a, 1999b; Schwartz et al., 2015). However, to our knowledge, previous studies have not investigated the effects of fire severity, post-fire climate, and topographic factors on vegetation recovery across a large spatial-temporal scale.

In this study, we examined effects of fire severity, post-fire climate, and topographic factors on short-term (<5 years) vegetation recovery in mixed-conifer and red fir forests in the Sierra Nevada. Normalized Difference Vegetation Index (NDVI) was used to monitor post-fire vegetation recovery trajectories (Clemente, Cerrillo, & Gitas, 2009; Epting & Verbyla, 2005; Henry & Hope, 1998; Hope, Tague, & Clark, 2007; Lee & Chow, 2015; Solans Vila & Barbosa, 2010). Competition between shrubs and trees starts immediately following fire in the Sierra Nevada (Collins & Roller, 2013; Crotteau et al., 2013; Nagel & Taylor, 2005), so vegetation recovery in this study refers to both tree and shrub regeneration. We used our analysis to explore two hypotheses:

(1) We hypothesized that short-term vegetation recovery patterns as measured by NDVI should be different among various fire severity patches, especially between low-moderate and high severity patches, considering the strong effects of fire severity on post-fire vegetation recovery (Chappell & Agee, 1996; Crotteau et al., 2013; Donato et al., 2009; Russell et al., 1998).
(2) We hypothesized that post-fire climate had significant impacts on short-term vegetation recovery as measured by NDVI in mixed-conifer forest at lower elevation (lower montane forest) and red fir forest at higher elevation (upper montane forest).

2. Methods

2.1. Study area

The study area encompassed the extent of two Landsat TM tiles, covering the central portion of the Sierra Nevada mountain range with an area of about 46,500 km^2 (Fig. 1). This region has a Mediterranean climate, with cool, moist winters and warm, dry summers. Most of the annual precipitation is in winter, and in the form of snow at higher elevation (above 1800 m). The native vegetation varies with elevation from chaparral shrubland communities at lower elevation (~380 to 1500 m), mixed conifer forest at mid-elevations (~1100 to 1900 m), and lodgepole pine and red fir forests (~2400 to 3000 m) to subalpine forest and alpine meadows at higher elevations (above around 2650 m) (Storer & Usinger, 1963). This study will focus solely on mixed-conifer and red fir forests derived from the 1977 Classification and Assessment with Landsat of Visible Ecological Groupings (1977 CALVEG, described below). Mixed-conifer forest primarily consist of white fir (*Abies concolor*), Douglas-fir (*Pseudotsuga menziesii*), sugar pine (*Pinus lambertiana*), ponderosa pine (*Pinus ponderosa*), Jeffrey pine (*Pinus jeffreyi*), incense-cedar (*Calocedrus decurrens*), California black oak (*Quercus kelloggii*), and other hardwood species (Collins & Roller, 2013). Mean fire return interval generally increases with elevation, which is a characteristic of the Sierra Nevada fire regime (Swetnam, Baisan, Morino, & Caprio, 1998).

2.2. Datasets

The main dataset applied to characterizing vegetation recovery following fire was based on 30-meter spatial resolution Landsat Time Series Stacks (LTSS) covering the period from 1994 to 2011. LTSS were preprocessed for radiometric normalization and masking of cloud and cloud shadow (Huang, Goward et al., 2010a; Huang, Thomas et al., 2010b). In order to remove potential errors caused by misregistration and terrain relief, each image in the LTSS was registered and orthorectified precisely using a corresponding base image with minimal geolocation errors and a digital elevation model (DEM) (Huang, Goward et al., 2010a). Preprocessing of data used in the LTSS was done through the Landsat Ecosystem Disturbance Adaptive Processing System (LEDAPS) (Gao, Masek, & Wolfe, 2009).

Corresponding maps of forest disturbance history (1984 to 2011) were generated by Vegetation Change Tracker (VCT), an automated algorithm for reconstructing forest disturbance history (Huang, Goward et al., 2010a). Based on the spectral-temporal properties of land cover and forest change processes, VCT disturbance maps record the changes in forests occurring over a particular year, while not providing detailed information on the disturbance type (Huang et al., 2009; Huang, Goward et al., 2010a). The Landsat imagery used for annual NDVI calculation (described below) was also derived from VCT. MTBS (Monitoring Trends in Burn Severity; http://www.mtbs.gov/) data were used to

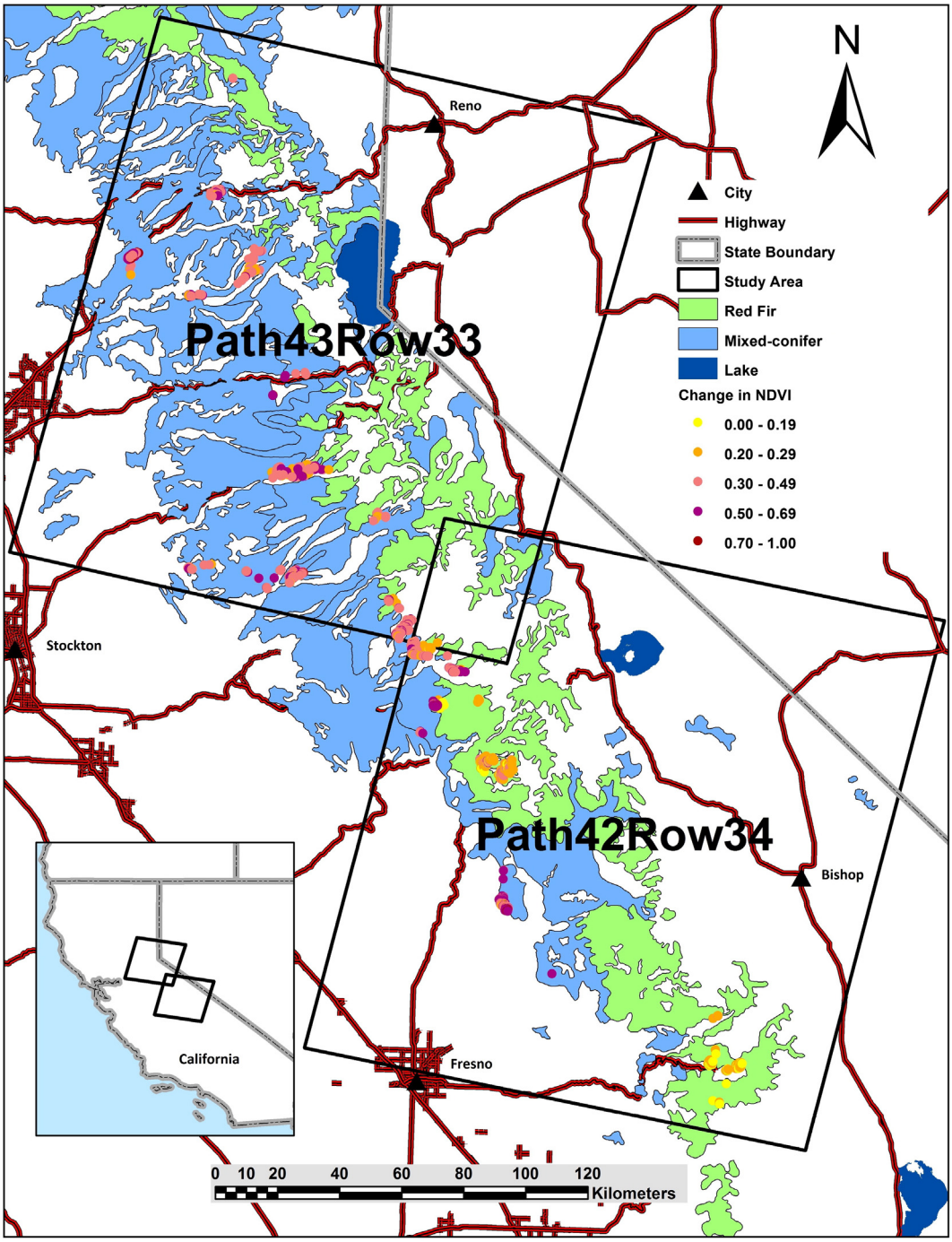

Fig. 1. A map showing the two Landsat tiles used for this study, along with mixed-conifer and red fir forest areas as classified by 1977 CALVEG; change in NDVI of burned pixels from Year +1 to Year +5 within the mixed-conifer and red fir forests is overlaid (see Section 3.1 below).

supplement the VCT disturbance maps. Within the study region, fires larger than 405 ha (1000 acres) were available in the MTBS dataset.

A 30-meter spatial resolution DEM (Digital Elevation Model) for the study area was acquired from the SRTM (Shuttle Radar Topography Mission) website (http://www2.jpl.nasa.gov/srtm/). Elevation, slope, and aspect variables were derived from the DEM. Climate data — monthly mean precipitation, January minimum temperature, and July maximum temperature — covering the 1972–2011 period were downloaded from the PRISM (Parameter-elevation Regressions on Independent Slopes Model) website (http://www.prism.oregonstate.edu/). PRISM makes use of point measurements of precipitation and temperature to generate continuous digital grid estimations for climate data with a 4-kilometer spatial resolution (Daly, Neilson, & Phillips, 1994). Wet season precipitation was calculated as the total precipitation modeled by PRISM for the months of December through May. Minimum and maximum temperature values represent the average of minimum and maximum daily temperatures modeled by PRISM during each month; January and July were selected as climatological extremes. Note that one 4-kilometer PRISM pixel encompassed many 30-meter LTSS pixels, providing a single PRISM climate variable value across those 30-meter pixels.

Recovery from fires that occurred from 1999 through 2006 was examined in this study, so a map of vegetation type coincident with or prior to 1999 was needed to target pre-fire mixed-conifer and red fir

forest types. The 1977 CALVEG is a statewide classification system developed by the US Forest Service, based on 1:250,000 scale Landsat Multispectral Scanner (MSS) imagery acquired between 1977 and 1979 (Parker & Matyas, 1979). The chance of dramatic changes in targeted forest prior to 1999 was greatly reduced by VCT. VCT was used to identify pixels that did not experience disturbance prior to 1999 or subsequent to 2011. Although the LTSS used for VCT starts from 1984, VCT is assumed to be able to capture "pre-series" disturbances before 1984 (Huang et al., 2009).

CALVEG is a hierarchical system originally derived from 6 formation categories (forest, woodland, chaparral, shrub, herbaceous and non-vegetated units). Through identifying distinctions among canopy reflectance values of Landsat MSS imagery, field verification, and professional guidance across the state, an initial 129 vegetation type series in eight regions of California were mapped and expanded to the current 213 types in nine regions. Vegetation forms of different ecological zones in the Sierra Nevada tend to correspond with elevation (Wagtendonk & Fites-Kaufman, 2006). 1977 CALVEG allowed comparison of post-fire vegetation recovery between two ecological zones (lower montane forest vs. upper montane forest) captured by the mixed-conifer and red fir forest classes, respectively.

2.3. Analysis methods

2.3.1. Stratification of NDVI time series for pixels burned in wildfires

We examined 35 fires larger than 405 ha occurring between 1999 to 2006 within the study area (Table A.1), and analyzed NDVI values 5 years before and after the fires (1994–2011). Increasing NDVI following fire was assumed to represent increasing cover of tree, shrub, and herbaceous vegetation, but NDVI does not allow identification of specific recovering vegetation types or species. Rapid vegetation recovery and dramatic changes in species composition and cover tend to occur in the first few years following wildfire (Collins & Roller, 2013; Donato et al., 2009; Hope et al., 2007; Lee & Chow, 2015; Nagel & Taylor, 2005), and species densities can likely reach a steady state within 6 years in the Sierra Nevada (Conard, Jaramillo, & Cromack, 1985; Donato et al., 2009). As a result, NDVI 5 years following fire (Year +5 NDVI) was chosen to study short-term vegetation recovery. VCT did not classify disturbance and MTBS data were used to isolate pixels within the study area that were burned once between 1999 and 2006. Pixels used for analysis were also restricted to mixed-conifer and red fir forest types by the 1977 CALVEG data. The number of qualified burned pixels after masking procedures varied from year to year: no qualified pixels were available in 2000, whereas in 2001, 2003, 2004 and 2005 there were a large number of qualified pixels (Fig. 2).

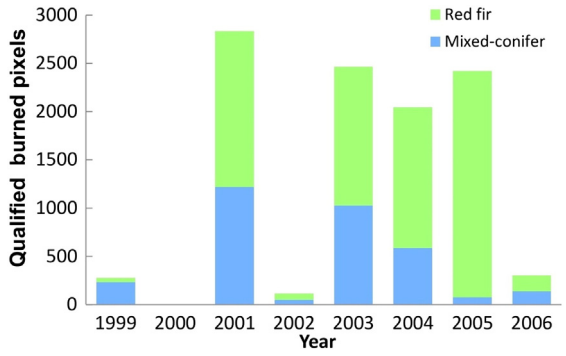

Fig. 2. Number of qualified burned pixels within two Landsat TM tiles covering the Sierra Nevada Mountains of California.

NDVI time series were calculated from the LTSS, according to Eq. (1) (Rouse, Haas, Schell, & Deering, 1974).

$$\mathrm{NDVI} = \frac{(R_{\mathrm{NIR}} - R_{\mathrm{Red}})}{(R_{\mathrm{NIR}} + R_{\mathrm{Red}})} \quad (1)$$

where R_{NIR} and R_{Red} represent surface reflectance for TM band 4 (760–900 nm) and band 3 (630–690 nm), respectively. For each burned pixel, an annual NDVI time series was constructed using the five pre-fire years (Years −5 through −1), the year of the fire (Year +0), and five post-fire years (Years +1 through +5). One of the biggest shortcomings in the use of NDVI for measuring vegetation status is that NDVI can reach saturation in dense vegetation canopies (Carlson, Perry, & Schmugge, 1990). In order to reduce the potential effects of saturation, we focused only on the early stages of vegetation recovery (up to 5 years) following fire. The post-fire vegetation recovery period in this study refers to NDVI values from Year +1 to Year +5 relative to fire.

2.3.2. Spatio-temporal modeling of vegetation recovery following fire

2.3.2.1. Variable definitions. To determine the environmental variables that were significantly correlated with post-fire vegetation recovery in mixed-conifer and red fir forests, OLS regression with spatial filtering (described below) was used to model NDVI values in Year +5. Topographic elements (elevation, slope, and aspect), climate variables (derived from PRISM), fire severity (derived from MTBS), the year when the fire occurred (hereafter 'disturbance year'), and Year +1 NDVI were used as predictor variables (Table 1).

The predictor variables used are described in Table 1 and were selected based on previous field studies (Collins & Roller, 2013; Crotteau et al., 2013; Goforth & Minnich, 2008; Russell et al., 1998; Shatford et al., 2007). Disturbance year was included as a dummy variable, due to potential variation in phenology across years. Rather than using a categorical variable to define the terrain aspect, we used two continuous variables called "northness" and "eastness" calculated using cosine and sine of aspect, respectively. Northness will be close to 1 if the aspect is generally north-facing and close to −1 if the aspect is generally south-facing. The eastness variable behaves similarly.

Relative differenced Normalized Burn Ratio (RdNBR) values of each fire case were derived from MTBS data and used directly as a proxy for fire severity (Miller & Thode, 2007; Miller, Knapp et al., 2009a). RdNBR is a remote sensing index developed for capturing the spatial complexity of fire severity in the US (Miller & Thode, 2007). Based on two best available Landsat images before and after fire, MTBS calculated the RdNBR values for each fire case. RdNBR-based thresholds for fire severity classes were developed to classify fires across time and space in the US (Miller & Thode, 2007; Miller, Knapp et al., 2009a). RdNBR has been shown to be correlated with field-measured fire severity, and past efforts to validate RdNBR have included several fires used in this study. Miller and Thode (2007) compiled fire severity data from 14 fires in the Sierra Nevada region and found an R-squared value of 0.61 field-measured severity. Four of 14 fires in Miller and Thode (2007) overlapped with this study (ID numbers 19, 20, 21, and 26 in Table A.1). Based on 30 fires, Miller, Knapp et al. (2009a) reported user's and producer's accuracies for RdNBR-based high fire severity classification ranging between 70.7% and 85.3%. Eight of 30 fires in Miller, Knapp et al. (2009a) overlapped with this study (ID numbers 7, 12, 14, 17, 19, 20, 21, and 26 in Table A.1).

Year +1 NDVI was incorporated into the model and used as a proxy for post-fire vegetation condition (i.e. open growing conditions and remnant tree overstory) (Collins & Roller, 2013; Donato et al., 2009). Open growing conditions can benefit the pioneer shrub species through more access to sunlight; remnant tree overstory can potentially produce higher shade and provide a seed source promoting higher densities of tree seedlings, thus limiting shrub competition (Crotteau et al., 2013).

Table 1
List of dependent and predictor variables considered in OLS regression.

Variable		Units	Description
Dependent variable	Year +5 NDVI	NDVI × 10,000	Continuous variable, a proxy for post-fire vegetation recovery status, 5-year post-fire
Burn effects	Year +1 NDVI	NDVI × 10,000	Continuous variable, a proxy for fire legacies
	RdNBR	RdNBR × 10,000	Continuous variable, a proxy for fire severity
Topography	Elevation	m	Continuous variable, the elevation of the burned pixel
	Slope	Degrees	Continuous variable, the slope of the burned pixel
	Northness		Continuous variable, calculated using cosine of aspect
	Eastness		Continuous variable, calculated using sine of aspect
Climate	Wet season precipitation anomaly in Year +0, Year +1, and the average anomaly of from Year +0 to Year +4	Z value	Continuous variable, total precipitation deviations in December, January, and February, March, April, and May in wet season following fire based on 40 years' observations (1972–2011)
	January minimum temperature anomaly in Year +0, Year +1, and the average anomaly from Year +0 to Year +4	Z value	Continuous variable, minimum temperature deviations in January following fire from 40 years' observations (1972–2011)
	July maximum temperature anomaly in Year +0, Year +1, and the average anomaly from Year +0 to Year +4	Z value	Continuous variable, maximum temperature deviations in July following fire from 40 years' observations (1972–2011)
Other	Disturbance year	Year	Dummy variable (Year 1999, Year 2001 … Year 2006)

Year +1 NDVI was selected over immediate post-fire (Year +0) NDVI due to the possibility of continued declines in NDVI in the year following fire disturbance. As a consequence of wildfire, vegetation sometimes gradually dies off in the post-fire period after surviving the direct burn (Solans Vila & Barbosa, 2010). Dramatic changes in species composition can occur and thus cause variations in NDVI during the post-fire period (Epting & Verbyla, 2005; Hope et al., 2007). Changes in surface reflectance following fire caused by leaching charcoals and burned remains can also result in post-fire changes in NDVI (White et al., 1996). In this study, the VCT algorithm may not discriminate consecutive multiple disturbances (i.e. post-fire salvage logging). If a wildfire is followed by salvage logging, lower NDVI values in Year +1 than in Year +0 can be expected. Also, in addition to best available Landsat images during leaf-on seasons, composite images created by temporal interpolation were used by VCT (Huang, Goward et al., 2010a) if necessary. As a result, Year +1 NDVI, rather than Year +0 NDVI, was used to reduce these potential effects.

Based on the 40-year (1972–2011) climate record, pixel-wise climate anomalies (z-scores) for wet season precipitation, January minimum temperature, and July maximum temperature were calculated (Eq. (2)).

$$z = \frac{X - \mu}{\sigma} \tag{2}$$

where X is the raw value, μ is the mean, and σ is the standard deviation. These standardized values can be used for directly comparing fires that occurred in different years and locations, and emphasize extreme values (Arnold, Brewer, & Dennison, 2014). Prior to climate anomaly calculation, an additional $\log_{10}$ transformation was performed on the wet season precipitation to normalize the skewed distribution. Post-fire climate anomalies in Year +0, Year +1, and the average anomaly from Year +0 to Year +4 were used as predictor variables to explain the variation in Year +5 NDVI (Table 1).

Modeling results showed that relationships between Year +5 NDVI and topographic slope in mixed-conifer and red fir forests were both significantly positive. Since steeper slopes tend to have shallow soil, rapid runoff, and higher fire severity (Lydersen & North, 2012; Kane, Lutz et al., 2015a), lower post-fire NDVI values were expected in high slope areas. We further investigated the relationship between slope and Year +5 NDVI observed in our study by comparing the pre-fire and post-fire NDVI and RdNBR values of low slope (<5°) and high slope (>25°) areas for mixed-conifer and red fir forests.

2.3.2.2. Model building. OLS with spatial filtering was used to determine the multiple environmental factors that were significant in explaining Year +5 NDVI. Linear models with spatial filtering were fitted separately for mixed-conifer and red fir forests using the combination of predictor variables in Table 1. As a global modeling technique, OLS regression models assume spatial stationarity (Mitchell & Yuan, 2010); the modeled OLS relationships are assumed to be constant across space (Miller & Hanham, 2011). The presence of spatial autocorrelation in change in NDVI values between Year +1 and Year +5 was tested for mixed-conifer and red fir forests through the global Moran's I statistics (Moran, 1950). The presence of spatial autocorrelation can violate the assumptions of OLS regression and severely affect the parameter estimates and error probabilities (Griffith, 2003).

According to the result of Moran's I, a regression model with spatial variation coefficients was necessary. Several spatial modeling techniques (e.g., spatial autoregressive, spatial filtering, Geographically Weighted Regression (GWR)) have been proposed to deal with the presence of spatial autocorrelation (Griffith & Peres-Neto, 2006; Lichstein, Simons, Shriner, & Franzreb, 2002; Rodrigues, de la Riva, & Fotheringham, 2014). We initially compared the performances of several spatial modeling techniques (Table A.2). In terms of model accuracy and dealing with spatial dependence, spatial filtering (Griffith & Peres-Neto, 2006) had the best performance. Eigenvector-based spatial filtering is a method that can characterize meaningful spatial forces by generating eigenvectors from a transformation procedure, depending on eigenfunctions of a matrix (Griffith & Peres-Neto, 2006). The generated eigenvectors, representing the dataset's spatial structure, can be incorporated into the OLS regression as additional predictor variables (Griffith, 2000; Griffith & Peres-Neto, 2006). Advantages of spatial filtering include reducing stochastic noise found in the residuals OLS modeling and increasing the normality and homoscedasticity of model residuals (Griffith, 2003; Thayn & Simanis, 2013). Compared to more conventional spatial autoregressive models, OLS with spatial filtering demonstrates higher fit statistics and provides a straightforward computation focus for dealing with spatial relationships in spatial modeling (Wang, Kockelman, & Wang, 2013). Eigenvector-based spatial filtering was implemented in the R environment with the spdep package (Bivand et al., 2011).

Due to the large number of qualified burned pixels (Fig. 2), random sampling was necessary to increase computational efficiency for OLS modeling with spatial filtering. According to Eq. (3) (Kotrlik & Higgins, 2001), the mean and standard deviation of the dependent variable population were calculated to estimate the necessary sample size (n). The margin value was estimated by calculating the mean difference in pre-fire NDVI values among disturbance years. At the 5% confidence

level (critical value 1.96), 30% and 40% of burned pixels, randomly selected, were estimated to represent the population of the dependent variable for mixed-conifer forest and red fir forest, respectively.

$$n = \left[\frac{z_{\frac{\alpha}{2}}\,\delta}{E}\right]^2 \quad (3)$$

where α is the confidence level, $z_{\alpha/2}$ is the corresponding critical value, δ is the standard deviation, and E is the margin value.

In order to ensure the robustness of relationship assessment between predictor variables and the dependent variable, we repeated the random sampling and OLS modeling with spatial filtering one hundred times, and then the frequency of each predictor variable with a significant relationship at the 95% level was counted. After dropping the predictor variables with low significant frequencies (<0.8), we repeated the whole process another one hundred times to ensure all predictor variables still had high significant frequencies. At the same time, the repetitive modeling results were summarized in terms of confidence interval at the 95% level. Model residuals were checked for normality and homoscedasticity. Pearson's correlation matrixes of predictor variables (except the dummy variable of disturbance year) and corresponding Variance Inflator Factor (VIF) for mixed-conifer and red fir forests were calculated to check for multi-collinearity (Craney & Surles, 2002).

2.3.3. Comparison of annual burned area fire severity with unburned areas

Frequency densities of NDVI values were calculated and used to compare vegetation recovery patterns between different fire severity classes and adjacent unburned areas. On the basis of 1977 CALVEG and VCT, mixed-conifer and red fir pixels lacking disturbance during the period 1984–2011 were randomly sampled from within a 4-kilometer radius of burned areas, consistent with the spatial resolution of the PRISM dataset. Such pixels shared the same pre-fire dominant vegetation cover type with the pixels inside the burned areas. Burned areas were stratified according to their fire severity (high, moderate, and low) by RdNBR values (Miller & Thode, 2007; Miller, Knapp et al., 2009a). Time-series frequency densities plots of NDVI values for mixed-conifer and red fir forests were subsequently generated to compare trajectories of post-fire vegetation recovery with fire severity.

3. Results

3.1. Post-fire vegetation recovery patterns

In the pre-fire period, the NDVI time series showed consistent values with low temporal variability, indicating stability in forest cover until the occurrence of fire (Fig. 3). In comparison to red fir forest, mixed-conifer forest generally tended to have higher pre-fire NDVI values. As expected, abrupt drops in mean NDVI in Year +0 following fires can be observed in both the red fir and mixed-conifer series. Although burned areas were generally characterized by increasing NDVI, the mean NDVI time series indicated pronounced differences in vegetation recovery between forest types and across fire years. NDVI decreased Year +0 to Year +1 for mixed-conifer (e.g., fire years 2001, 2002, and 2006) and red fir forests (e.g., fire years 2002 and 2003). The NDVI time series of both forest types also indicated a higher temporal variability in the post-fire period than in the pre-fire period for most disturbance years (Table 2). Nevertheless, all of the NDVI series indicated a general trend toward pre-fire values following fire (Fig. 3).

Before modeling post-fire NDVI values, we investigated the spatial patterns of NDVI values for burned pixels (Fig. 1). Change in NDVI from Year +1 to Year +5 (i.e. NDVI in Year +5–NDVI in Year +1) tended to be spatially clustered, signifying strong spatial effects. Changes in NDVI also tended to be lower in red fir forest than in mixed-conifer forest. Positive Moran's I index values (0.33 and 0.62 for mixed-conifer and red fir, respectively) with z-scores of 153.39 ($p < 0.001$) and 82.47 ($p < 0.001$) confirmed a tendency toward spatial clustering of change in NDVI values between Year +1 and Year +5. These results indicated that the relationship between the predictor variables and the dependent variable in the OLS models can vary across geographic space, and a spatial modeling technique is necessary to deal with spatial structures in the datasets.

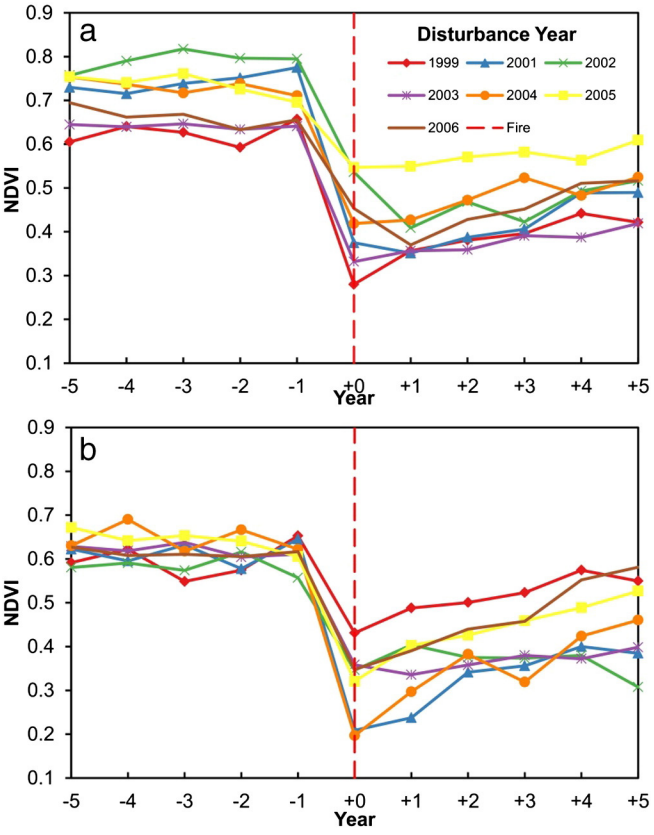

Fig. 3. Time-series mean NDVI values by disturbance year a. Mixed-conifer forests b. Red fir forests.

3.2. Relationships between environmental factors and post-fire vegetation recovery

Average anomalies of post-fire climate variables over Years +0 through +4 were not used in modeling because of their strong multicollinearity with post-fire climate anomalies in Year +0 and Year +1. Strong relationships were found between Year +5 NDVI and five predictor variables (Year +1 NDVI, slope, disturbance year, fire severity,

Table 2
Standard deviations of NDVI values for pre-fire and post-fire periods for each disturbance year.

Disturbance year	Pre-fire period (mixed-conifer)	Post-fire period (mixed-conifer)	Pre-fire period (red fir)	Post-fire period (red fir)
1999	0.026	0.057	0.041	0.050
2001	0.023	0.059	0.028	0.079
2002	0.022	0.051	0.022	0.033
2003	0.005	0.031	0.014	0.022
2004	0.017	0.045	0.032	0.096
2005	0.026	0.023	0.024	0.072
2006	0.022	0.054	0.009	0.091

Table 3
Frequencies of predictor variables with a significant estimation at the 95% level after repetitive OLS with spatial filtering run one hundred times.

Variable	Frequency (mixed-conifer)	Frequency (red fir)
Year +1 NDVI	100	100
Elevation	13	100
Slope	93	100
Northness	95	15
Eastness	27	98
Year +0 Wet season precipitation anomaly	87	21
Year +1 Wet season precipitation anomaly	17	24
Year +0 January minimum temperature anomaly	100	96
Year +1 January minimum temperature anomaly	28	57
Year +0 July maximum temperature anomaly	2	64
Year +1 July maximum temperature anomaly	0	8
Disturbance year	100	100
Fire severity	100	100

and Year +0 January minimum temperature anomaly) for both mixed-conifer and red fir forests (Table 3). Northness and Year +0 wet season precipitation anomaly were only robust for explaining variations in Year +5 NDVI for mixed-conifer forest, and eastness and elevation were only robust for explaining variations in Year +5 NDVI for red fir forest.

The OLS regressions with spatial filtering shown in Eqs. (4) and (5) were adopted after dropping predictor variables with low significance frequency (<80) (Table 3). In the following equation, β0 is the intercept and β1 to β6 are the coefficients; $\beta_{\text{Disturbance year}}$ is the dummy variable, and ε is the residual:

$$\begin{aligned}\text{Year}+5\ \text{NDVI for mixed-conifer} &= \beta 0+\beta 1\text{Year}+1\ \text{NDVI}+\beta 2\text{Slope}\\ &+\beta 3\text{Northness}+\beta 4\text{Year}+0\ \text{Wet season precipitation anomaly}\\ &+\beta 5\text{Year}+0\text{January minimum temperature anomaly}\\ &+\beta 6\ \text{Fire severity}+\beta_{\text{Disturbance year}}+\varepsilon\end{aligned} \quad (4)$$

$$\begin{aligned}\text{Year}+5\ \text{NDVI for red fir} &= \beta 0+\beta 1\text{Year}+1\ \text{NDVI}+\beta 2\text{Slope}\\ &+\beta 3\text{Eastness}+\beta 4\text{Elevation}+\beta 5\text{Year}\\ &+0\ \text{January minimum temperature anomaly}+\beta 6\ \text{Fire severity}\\ &+\beta_{\text{Disturbance year}}+\varepsilon\end{aligned} \quad (5)$$

We summarize the repetitive modeling results for mixed-conifer and red fir forests in Tables 4 and 5, respectively. The modeling results are shown in terms of confidence interval at the 95% level, based on the repetitive random sampling and OLS modeling for one hundred times. All of the aforementioned variables for predicting Year +5 NDVI were statistically significant at the 95% level in Tables 4 and 5. In general, red fir forests (adjusted R-squared = [0.680, 0.688]) had a slightly better modeling performance than mixed-conifer forests (adjusted R-squared = [0.671, 0.678]).

Randomly selected pixels with all predictor variables significant at the 95% level, out of one of the repetitive random samplings, were used for partial regression plots and relative importance analysis of predictor variables. By holding values for other than the corresponding predictor variables constant, partial regression plots were used to characterize relationships between the Year +5 NDVI (dependent variable) and each predictor variable (Figs. A.1 and A.2, the dummy variable of disturbance year was not shown) in Eqs. (4) and (5) for each forest type (Cook, 2009).

With regards to the role of environmental factors, several lines of evidence attested to the strong relationship between Year +5 NDVI and predictor variables. The coefficient values and partial regression plots for the predictor variables revealed a positive relationship between Year +5 NDVI and two of the factors— slope and Year +1 NDVI for both red fir and mixed-conifer forests; in contrast, a negative relationship existed between Year +5 NDVI and fire severity. The dummy variable—disturbance year—was also significant for both forest types. Comparison of high (>25°) and low (<5°) slope areas suggested that differences in pre-fire vegetation status caused the slope relationship observed in mixed-conifer forest (Table 6). In contrast, the slope relationship in red fir forest might be attributed to differences in fire severity between low slope and high slope areas (Table 6).

Year +5 NDVI demonstrated different responses to some topographic and climate-related variables between mixed-conifer and red fir forests (Tables 4 and 5). There was a positive relationship between Year +5 NDVI and Year +0 January minimum temperature anomaly in red fir forest, while the opposite trend existed in mixed-conifer forest. In addition, positive wet season precipitation anomalies in Year +0 predicted greater NDVI values in Year +5 in mixed-conifer forest. One of the aspect-related variables—northness—was negatively related with Year +5 NDVI in mixed-conifer forest, and another aspect-related variable—eastness—was positively related with Year +5 NDVI in red fir forest. Also, the higher the elevation, the lower the expected Year +5 NDVI value in red fir forest.

The relative importance of each predictor variable for each forest type was explored in the R environment using the caret package (Kuhn, 2015). Specifically, each of the predictor variables was dropped sequentially from each model, and the drop in the absolute values of the t-statistics was used as a measure of relative importance (Kuhn, 2015). Fire severity was most important for explaining Year +5 NDVI in mixed-conifer forest (Fig. 4). Post-fire climate variables (Year +0 January minimum temperature anomaly and Year +0 Wet season precipitation anomaly) also had high relative importance values in mixed-conifer forest. In contrast, the post-fire climate variable Year +0 January minimum temperature anomaly had much less

Table 4
Repetitive OLS modeling results for mixed-conifer forests with spatial filtering, in terms of confidence interval at the 95% level[a].

Variable	Coefficient	Std. error	t-Statistics
Intercept	[4252.026,4309.876]	[107.263–109.031]	[39.252, 40.033]
Fire severity	[−1.025, −0.975]	[0.078, 0.080]	[−12.893, −12.383]
Year +1 NDVI	[0.089, 0.096]	[0.013,0.014]	[6.523,7.022]
Slope	[11.350, 12.716]	[2.400, 2.432]	[4.700, 5.252]
Year +0 January minimum temperature anomaly	[−5.004, −4.682]	[0.650, 0.660]	[−7.638, −7.156]
Year +0 wet season precipitation anomaly	[154.616, 161.745]	[16.483, 16.701]	[9.317, 9.774]
Northness	[−175.489, −158.980]	[30.322, 30.720]	[-5.757, −5.213]
Factor(Year 2001)	[648.272, 691.350]	[82.012, 83.340]	[7.841, 8.400]
Factor(Year 2002)	[1079.112, 1223.543]	[275.438, 296.987]	[3.865, 4.411]
Factor(Year 2003)	[−166.798, −130.991]	[30.322, 37.057]	[−2.191,1.720]
Factor(Year 2004)	[812.387, 858.936]	[84.637, 85.959]	[7.522, 8.121]
Factor(Year 2005)	[1535.266, 1671.782]	[440.804, 493.831]	[3.438, 3.821]
Factor(Year 2006)	[356.478, 860.197]	[118.206, 161.115]	[3.838,4.735]

[a] Coefficients values based on scaled NDVI by 10,000; Residual standard error = [648.558, 655.302]; Multiple R-squared = [0.691, 0.699]; Adjusted R-squared = [0.671, 0.678].

Table 5
Repetitive OLS modeling results for red fir forests with spatial filtering, in terms of confidence interval at the 95% level[a].

Variable	Coefficient	Std. error	t-Statistics
Intercept	[7392.183, 7636.413]	[390.555, 408.900]	[18.537, 19.545]
Fire severity	[−0.463, −0.427]	[0.0750, 0.0760]	[−6.141, −5.654]
Year +1 NDVI	[0.194, 0.203]	[0.017, 0.018]	[11.152, 11.642]
Slope	[13.880, 15.294]	[2.802, 2.839]	[4.926, 5.428]
Year +0 January minimum temperature anomaly	[167.832,187.668]	[45.457, 46.013]	[3.669, 4.102]
Elevation	[−1.448, −1.397]	[0.109, 0.110]	[−13.247, −12.748]
Eastness	[140.160, 152.068]	[28.377, 28.711]	[4.911, 5.333]
Factor (Year 2001)	[−339.698, −104.840]	[307.553, 330.001]	[−1.056, −0.364]
Factor (Year 2002)	[−2079.174, −1830.554]	[350.296, 371.367]	[−5.874, −5.162]
Factor (Year 2003)	[−1090.762, −853.424]	[294.206, 317.427]	[−3.660, −2.903]
Factor (Year 2004)	[−295.724, −60.642]	[297.777, 320.771]	[−0.949, −0.233]
Factor (Year 2005)	[−190.060, −37.849]	[295.812, 318.896]	[−0.605, 0.121]
Factor (Year 2006)	[665.807, 904.538]	[316.562, 338.395]	[2.116, 2.815]

[a] Coefficients values based on scaled NDVI by 10,000; Residual standard error = [656.678, 663.936]; Multiple R-squared = [0.697, 0.704]; Adjusted R-squared = [0.680, 0.688].

power for explaining Year +5 NDVI in red fir forest. Elevation had the largest relative importance value in red fir forest instead. For red fir forests, Year +1 NDVI had a higher relative importance value compared to fire severity. Landscape position variables (northness, eastness, and slope) had the similar relative importance values in mixed-conifer and red fir forests. The dummy variable (disturbance year) was a more important predictor variable in mixed-conifer forest than in red fir forests.

Similar to Fig. 3, abrupt changes in NDVI can be observed in frequency densities in Year +0 following fire for both mixed-conifer and red fir forests (Fig. 5). Burned pixels didn't recover to pre-fire status during 5 years following fire, although differences between unburned and burned areas decreased over time. NDVI values in the high severity group were lower than in low and moderate severity groups in Year +0. Fire severity effects in mixed-conifer forest were apparent in Year +0, but disappeared quickly starting from Year +1; in contrast, apparent fire severity effects in red fir forest persisted for a longer time from Year +0 to Year +5, although they also diminished over time.

3.3. Model diagnostics

No strong multi-collinearity appeared to exist among predictor variables for each forest type model as assessed by VIF (Tables 7, 8). VIF values in the red fir model tended to be larger than in the mixed-conifer model, but still smaller than the VIF threshold value of 10 commonly used for diagnosing collinearity (O'Brien, 2007). Moreover, except the moderate correlation between the fire severity (RdNBR) and Year +1 NDVI variables for each forest type (−0.209 and −0.353 respectively), as well as Year +0 January minimum temperature anomaly and slope for red fir forests (0.328), most of the correlations between predictor variables were very weak. By checking model residuals, we also did not find clear violation of normality and homoscedasticity (Figs. A.3, A.4).

Modeling results of OLS with spatial filtering show a large improvement compared to the results of OLS alone, in terms of accuracy and adjusted R-squared. Adjusted R-squared increased from 0.319 to 0.676 for mixed-conifer and from 0.442 to 0.687 for red fir. Accordingly, residual standard error decreased from 976.9 to 649.9 for mixed-conifer and from 871.2 to 658.1 for red fir. Also, spatial autocorrelation among predictor variables was filtered out for each forest type model: Moran's I decreased and became non-significant (0.412 to 0.104 for mixed-conifer, 0.322 to 0.081 for red fir, $p < 0.001$).

Table 6
Mean NDVI and RdNBR values of low-slope (<5°) and high slope (>25°) pixels.

	Mean Year −1 NDVI (NDVI × 10,000)	Mean Year +5 NDVI (NDVI × 10,000)	RdNBR (RdNBR × 10,000)
Mixed-conifer forests			
Low slope (<5°)	6245	4418	531
High slope (>25°)	7582	5154	666
Red fir forests			
Low slope (<5°)	6211	3833	845
High slope (>25°)	5995	4868	649

4. Discussion

The modeling results (Tables 3–5) indicate that climate conditions in the first post-fire growing seasons (Year +0) might be one of the most important factors for vegetation recovery in the Sierra Nevada. Higher Year +5 NDVI values in mixed-conifer forest were associated with higher Year +0 wet season precipitation, in correspondence with the general spatial pattern that water stress decreases with elevation in lower montane forests of the Sierra Nevada (Miller & Urban, 1999b). Post-fire drought is unfavorable for tree regeneration after disturbances in Mediterranean environments (Broncano & Retana, 2004; Chappell & Agee, 1996; Daskalakou & Thanos, 1996; Sánchez-Gómez, Valladares, & Zavala, 2006). Enough moisture from immediate surroundings is important for post-disturbance seed germination (Minore & Laacke, 1992; Tappeiner, Newton, McDonald, & Harrington, 1992).

January minimum temperature was significant for explaining post-fire NDVI values in both mixed-conifer and red fir forests. The negative temperature relationship for mixed-conifer forest could be a proxy for drought effects, but the positive relationship for red fir forest could be related to high elevation limitations of solar radiation and temperature on vegetation growth (Greenberg, Dobrowski, & Vanderbilt, 2009; Miller & Urban, 1999b). Although having a small direct effect, favorable temperature can become a critical factor, when enough moisture is available (Minore & Laacke, 1992). An inverse relationship between elevation and Year +5 NDVI was found for red fir forest, which can be probably also attributed to the decreased temperature with elevation in upper montane forests of Sierra Nevada (Miller & Urban, 1999b).

In terms of relative importance of predictor variables, post-fire climate variables (Year +0 January minimum temperature anomaly and Year +0 wet season precipitation anomaly) had high predictive powers in mixed-conifer forest, secondary to fire severity. Year +0 January minimum temperature anomaly in red fir forest was not as important as in mixed-conifer forest. Elevation had the largest predictive power

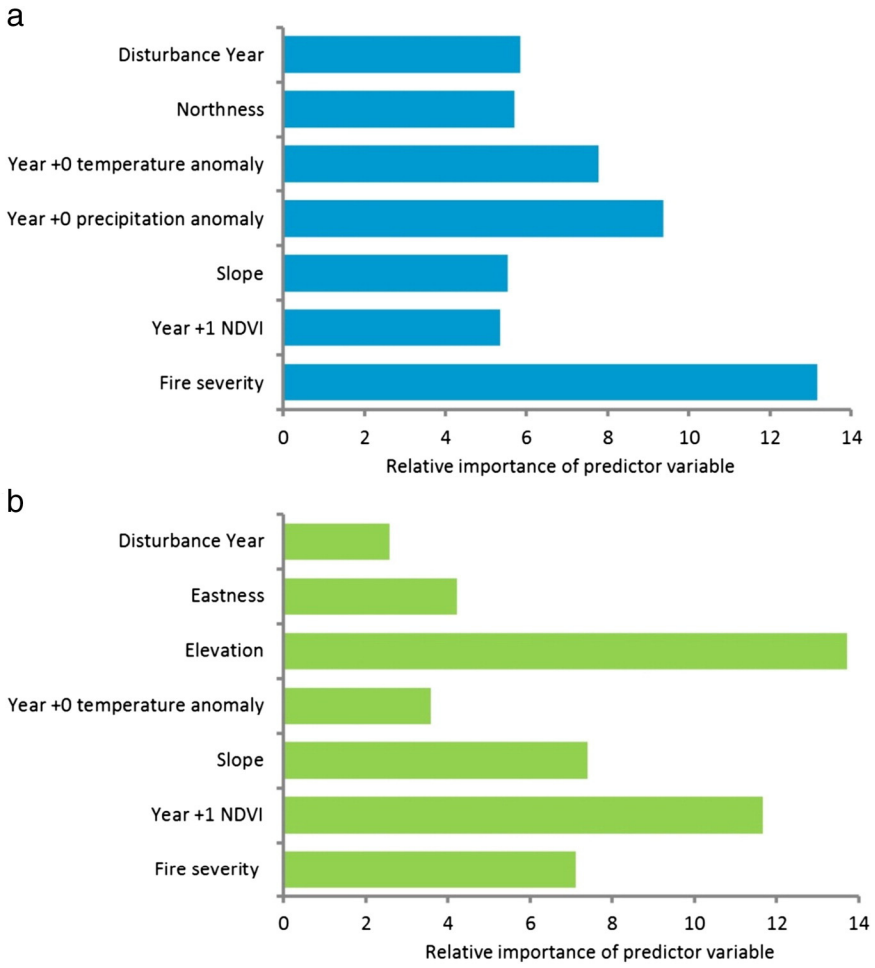

Fig. 4. Relative importance of predictor variables for (a) Mixed-conifer forests, and (b) Red fir forests.

among all predictor variables for red fir forest. These findings as well as the empirical relationships found in the models together suggest that, in our study area, vegetation recovery in mixed-conifer forest at lower elevation may be more sensitive to post-fire drought, but vegetation recovery in red fir forest at higher elevation, where soil moisture is less of a limiting factor, may be more sensitive to post-fire temperature. In the

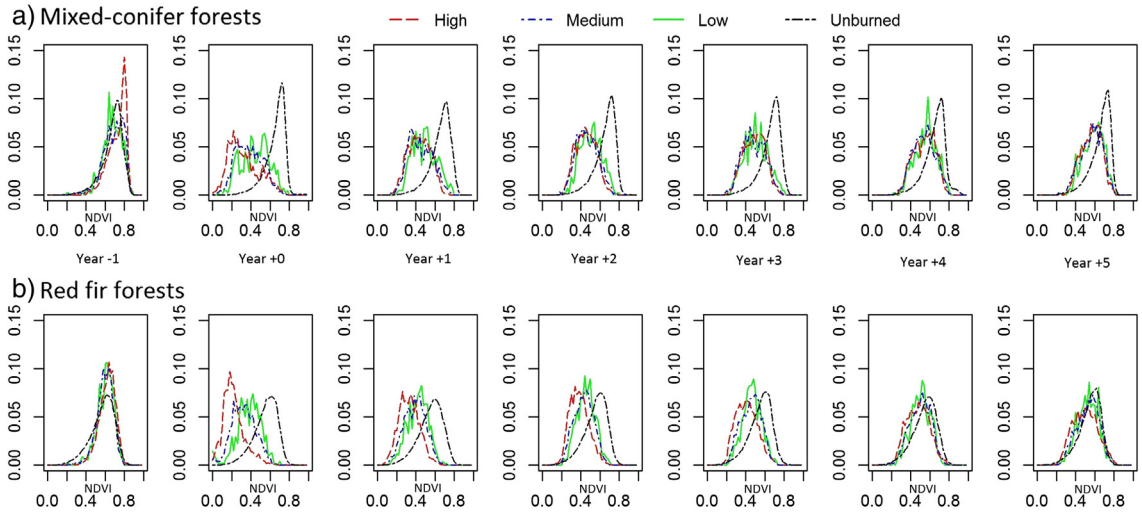

Fig. 5. Frequency distributions of NDVI values by fire severity a. Mixed-conifer forests b. Red fir forests.

Table 7
Pearson correlation matrixes of predictor variables and corresponding VIF for mixed-conifer forests.

	RdNBR	Year +1 NDVI	Slope	Year +0 Wet season precipitation anomaly	Year +0 January minimum temperature anomaly	Northness
RdNBR	1	−0.209	0.136	−0.096	−0.129	0.010
Year +1 NDVI		1	−0.064	−0.172	0.172	−0.064
Slope			1	−0.104	−0.139	0.064
Year +0 Wet season precipitation anomaly				1	−0.071	−0.072
Year +0 January minimum temperature anomaly					1	−0.034
Northness						1
VIF	1.187	1.367	1.384	1.410	1.326	1.169

future, stratified field sampling can be set up to account for the effects of post-fire drought across a large spatial-temporal domain, based on the results of this study.

The climate data used in this study had a coarser resolution compared to Landsat and topographic data. The consequent scale mismatch between environmental and climate data might result in decreased explanation of spatial variation and underestimation of relationships among other predictor variables, and thus added to model uncertainty on multi-collinearity (Borcard, Legendre, Avois-Jacquet, & Tuomisto, 2004; De Knegt et al., 2010; Diniz-Filho & Bini, 2005). The scale mismatch might also reduce the precision of coefficient estimation and obstruct inferential tests (De Knegt et al., 2010). Nevertheless, biased significance tests of regression coefficients caused by scale mismatch should be greatly reduced in this study, because eigenvector-based spatial filtering is designed to capture spatial structures at varying scales (Diniz-Filho & Bini, 2005). Partial regression plots still indicated the strong effects of post-fire climate on Year +5 NDVI values across the landscape (Figs. A.1 and A.2). Topographic data, especially elevation, were used for downscaling climate data in the PRISM model (Daly et al., 1994), so finer scale climate differences may be partially accounted for by including elevation in the OLS model.

Landscape position can also strongly influence post-fire vegetation recovery through its effects on local microclimate and hydrological processes (Ireland & Petropoulos, 2015; Mitchell & Yuan, 2010). Regression models in this study showed that north-facing aspects in mixed-conifer forest tended to have higher post-fire vegetation cover compared to south-facing exposures. This is consistent with studies (within the northern hemisphere) showing that south-facing aspects were more prone to drought, and therefore recovery appeared to be slower compared to north-facing aspects (Ireland & Petropoulos, 2015; Malkinson, Beeri, Halutzy, & Tesler, 2007; Mitchell & Yuan, 2010). In red fir forest, east-facing aspects exhibited significantly higher post-fire vegetation cover compared to west facing exposures. Further investigation is necessary to explain this relationship and relationships between slope, fire severity, and post-fire vegetation recovery.

While NDVI values have a strong increasing trend in the years following fire, field studies have shown that it may take several decades for burned sites to recover to pre-fire status (Collins & Roller, 2013; Russell et al., 1998; Taylor & Halpern, 1991). Corresponding to results from field-based studies in the Sierra Nevada and southern Cascades (Collins & Roller, 2013; Crotteau et al., 2013), the effects of fire severity on post-fire NDVI were still notable 5 years following fire (Fig. 5), and lower Year +5 NDVI values were found for high-severity burn areas (Tables 4 and 5). In addition, differences in burn effects within fire severity patches tend to become smaller over time in terms of NDVI (Fig. 5). But compared to mixed-conifer forest at lower elevation, NDVI differences between fire severity patches are be more persistent in red fir forest at higher elevation (Fig. 5). This is likely due to the heavy snow, longer winter, and shorter growing season at high elevations where red fir forests are found (Laacke & Tappeiner, 1996).

In the Sierra Nevada, a number of plot-based studies have observed that post-fire vegetation recovery during the early succession period can be characterized by the competition between tree and shrub species, especially in high-severity patches (Collins & Roller, 2013; Crotteau et al., 2013; Kauffman & Martin, 1990, 1991; Nagel & Taylor, 2005). High shrub seedling mortality has been also observed in the Sierra Nevada in the first few years following germination, especially when tree seedlings overtop shrub seedlings (Conard et al., 1985). Reestablishment of tree species is often a forest management priority following wildfire. In similar Mediterranean ecosystems, some studies indicate that shrub species can act as “nurse” plants that promote the success of forest regeneration in the long run (Castro, Zamora, Hódar, & Gómez, 2002; Castro, Zamora, Hódar, Gómez, & Gómez-Aparicio, 2004; Dunne & Parker, 1999; Gómez-Aparicio et al., 2004). On the other hand, with increasing fire severity and drying trends in the western US (Miller, Safford, Crimmins, & Thode, 2009b; Westerling, Hidalgo, Cayan, & Swetnam, 2006), shrub species may be strong competitors and inhibit forest regeneration (Allen et al., 2010; Collins & Roller, 2013; Dale et al., 2001; Miller & Thode, 2007). In decades to come, however, ecosystem management may even struggle to maintain woody shrub

Table 8
Pearson correlation matrixes of predictor variables and corresponding VIF for red fir forests.

	RdNBR	Year +1 NDVI	Slope	Year +0 January minimum temperature anomaly	Elevation	Eastness
RdNBR	1	−0.353	−0.138	−0.113	0.102	−0.002
Year +1 NDVI		1	0.208	0.177	−0.010	0.043
Slope			1	0.328	−0.022	−0.088
Year +0 January minimum temperature anomaly				1	−0.068	0.017
Elevation					1	−0.083
Eastness						1
VIF	1.545	1.674	1.902	1.937	1.544	1.235

species across many currently forested areas, as conditions become markedly hotter and drier (e.g., Batllori, Ackerly, & Moritz, 2015; D'Antonio & Vitousek, 1992; Lenihan, Bachelet, Neilson, & Drapek, 2008).

A primary limitation of spectral vegetation indices based analysis is that recovery of specific vegetation types or species may not be identifiable (Meng, Dennison, D'Antonio, & Moritz, 2014). While satellite-based NDVI was used for determining vegetation recovery following fire, we recognize that short-term NDVI following wildfire represents relative vegetation cover rather than a direct measure of forest regeneration. Thus, we could not assess vegetation species (shrub and tree) composition and abundance in burned areas using the remote-sensing based methodology in this study. In the future, more efforts are needed to explore the long-term competition between forest and shrub species in burned areas using the increasing availability of remote sensing data or through stratified field samplings. For example, more comprehensive information at the species level can be derived from the fusion of very high spatial resolution, lidar, or hyperspectral data (Huesca et al., 2013; Kane et al., 2013, 2014; Polychronaki, Gitas, & Minchella, 2013).

The accuracy of MTBS (i.e. fire severity) and VCT (i.e. forest disturbance history) products constrained the quality and validity of the results in this study. NBR and its derivative indices may not be spectrally optimal for measuring fire severity (Roy, Boschetti, & Trigg, 2006), and some variation in severity may be difficult to capture with these indices (De Santis & Chuvieco, 2007, 2009; Roy et al., 2006). However, comprehensive accuracy assessments on RdNBR-based fire severity mapping in the study area have shown reliable results (Miller & Thode, 2007; Miller, Knapp et al., 2009a). The overall accuracy of VCT disturbance maps was found between 77% and 86% at the national scale (Thomas et al., 2011). Based on a pixel-based interpretation in Greater Yellowstone Ecosystems, the VCT fire detection was found to be highly reliable, with user's accuracy of 96% and producer's accuracy of 73% (Feng, Chengquan, & Zhiliang, 2015). With the emerging of a new generation of fire remote sensing products (Boschetti, Roy, Justice, & Humber, 2015; Csiszar et al., 2014; Parks, Dillon, & Miller, 2014), further improvements can be expected in post-fire recovery studies.

5. Conclusions

Due to the anticipated impacts of climate change on western US ecosystems, there is a considerable body of research concerning how climate change has and will impact forest structure, disturbance regimes, and carbon storage and dynamics (Allen et al., 2010; Bond-Lamberty et al., 2014; Dale et al., 2001; Dennison, Brewer, Arnold, & Moritz, 2014; Flannigan, Stocks, & Wotton, 2000; Moritz et al., 2012; Rogers et al., 2011; Schwartz et al., 2015). Our study provides insights into the mechanisms of environment-fire interactions on forest change by quantifying the relative contributions of multiple environmental factors in two types of Sierra Nevada forests. Given the expected increases in fire severity (Miller, Safford et al., 2009b) and drying trend (Westerling et al., 2006) as climate changes in western US ecosystems, we focused on the effects of fire severity and post-fire climate on vegetation recovery. The results in this study indicate that fire severity and post-fire climate might have significant effects on postfire vegetation recovery, but these effects might vary by ecological zone in the Sierra Nevada (lower montane forest vs. upper montane forest). Therefore, adaptive management guidelines for different forest ecosystems might be necessary under most climate change scenarios. Our results combined with longer-term monitoring may be useful for incorporation into a forest gap model (Miller & Urban, 1999a) or for calibrating ecosystem simulation models to gain a better understanding of the interactions between climate, disturbance and vegetation dynamics (Thonicke, Venevsky, Sitch, & Cramer, 2001; Thornton et al., 2002). Improved understanding of the mechanisms of environment-fire interactions on forest change will assist management efforts to protect and sustain the multiple resources valued in these ecosystems.

Acknowledgments

Funding for this research was provided by California Energy Commission grant 500-10-045. The authors would like to thank Feng A. Zhao for data assistance.

Appendix A

Table A.1
Name, ignition dates, and size of 35 fires included in the study.

ID	Fire name	Ignition date	Size (hectares)	ID	Fire name	Ignition date	Size (hectares)
1	ELEANOR	Aug 16, 1999	1,009	19	MOUNTAIN COMPLEX	Jul 20, 2003	1632
2	HIRAM	Aug 8, 1999	1,142	20	MUD WFU	Aug 31, 2003	1804
3	NORTH PARK COMPLEX	Aug 10, 1999	3,566	21	WHITT	Aug 31, 2003	461
4	SOUTH PARK COMPLEX	Jul 7, 1999	853	22	ARMSTRONG	Aug 6, 2003	437
5	BURNT	Jul 30, 2001	774	23	FREDS	Oct 13, 2004	3298
6	DARBY	Sep 5, 2001	5,963	24	HETCHY	Oct 15, 2004	832
7	GAP	Aug 12, 2001	6,688	25	MEADOW COMPLEX	Jul 1, 2004	2235
8	HOOVER COMPLEX	Jul 10, 2001	3,708	26	POWER	Oct 6, 2004	6987
9	LEONARD	Aug 18, 2001	2,131	27	STEVENS	Aug 8, 2004	395
10	NORTH FORK	Aug 20, 2001	1,681	28	COMB COMPLEX	July 17, 2005	24,904
11	PONDEROSA	Aug 27, 2001	1,240	29	PW-3 SEG 3	Oct 12, 2005	761
12	STAR	Aug 25, 2001	6,817	30	BASSETTS	Sep 19, 2006	939
13	PLUM	Nov 25, 2002	747	31	BL MAST WUI06	Sep 1, 2006	957
14	WOLF	Jul 11, 2002	754	32	CEDAR GROVE ROARING	Jul 2, 2006	3,053,991
15	DUNCAN COMPLEX	Jul 31, 2003	448	33	FROG	Jul 21, 2006	2700
16	KAWEAH-KERN COMPLEX	Jul 28, 2003	1,429	34	RALSTON	Sep 5, 2006	3227
17	KIBBIE COMPLEX	Jul 29, 2003	2,689	35	SOS 06	Dec 1, 2006	996
18	TUOLUMNE	Aug 31, 2003	1,360				

Table A.2
Performance comparison of different spatial modeling techniques in OLS regression.

	GWR	Spatial autoregressive	Spatial filtering
Mixed-conifer			
Adjusted R-squared	0.307	0.655	0.676
Residual Moran's I	0.399	0.116	0.104
Red fir			
Adjusted R-squared	0.483	0.566	0.687
Residual Moran's I	0.295	0.087	0.081

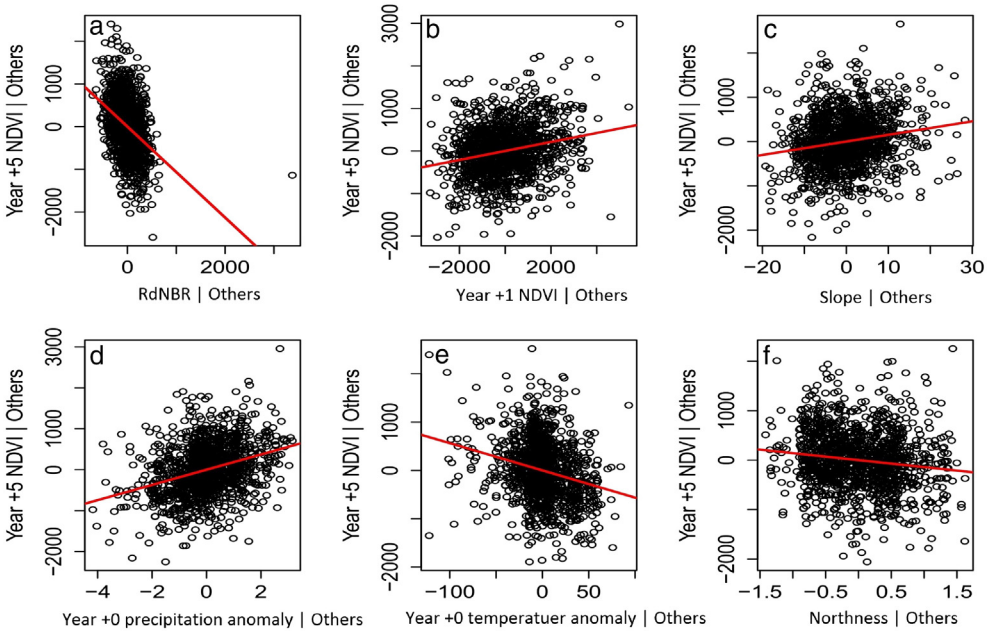

Fig. A.1. Partial regression plots of Year +5 NDVI against (a) RdNBR, (b) Year +1 NDVI, (c) slope, (d) Year +0 wet season precipitation anomaly, (e) Year +0 January minimum temperature anomaly, (f) Northness for mixed-conifer forests. The Y-axis of each panel shows the residuals from regressing the dependent variable against all predictor variables other than the corresponding predictor variable, and the X-axis of each panel shows the residuals from regressing the corresponding predictor variable against all the remaining predictor variables (Fox & Weisberg, 2010). The partial regression plots were implemented under R environment with the car package (Fox & Weisberg, 2010).

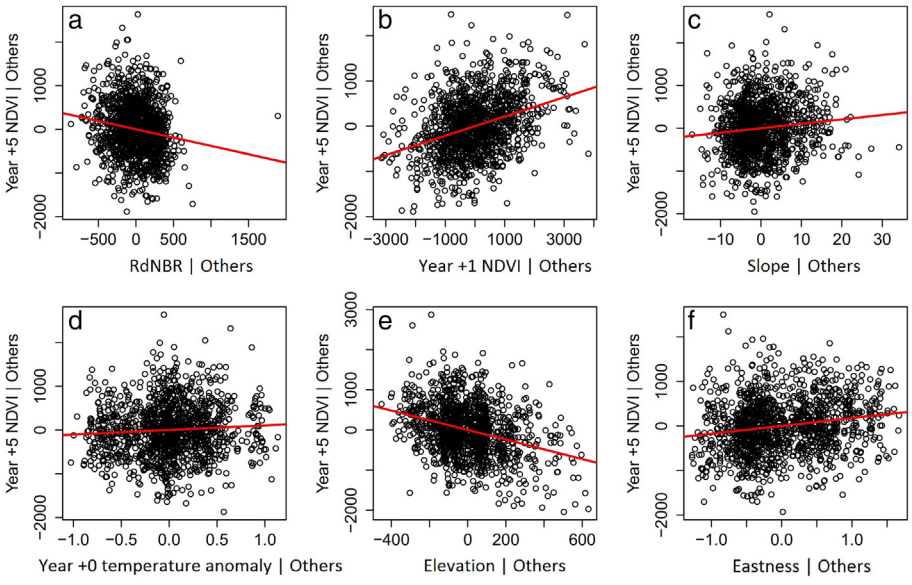

Fig. A.2. Partial regression plots of Year +5 NDVI against (a) RdNBR, (b) Year +1 NDVI, (c) slope, (d) Year +0 January minimum temperature anomaly, (e) Elevation, and (f) Eastness for red fir forests. The Y-axis of each panel shows the residuals from regressing the dependent variable against all predictor variables other than the corresponding predictor variable, and the X-axis of each panel shows the residuals from regressing the corresponding predictor variable against all the remaining predictor variables (Fox & Weisberg, 2010). The partial regression plots were implemented under R environment with the car package (Fox & Weisberg, 2010).

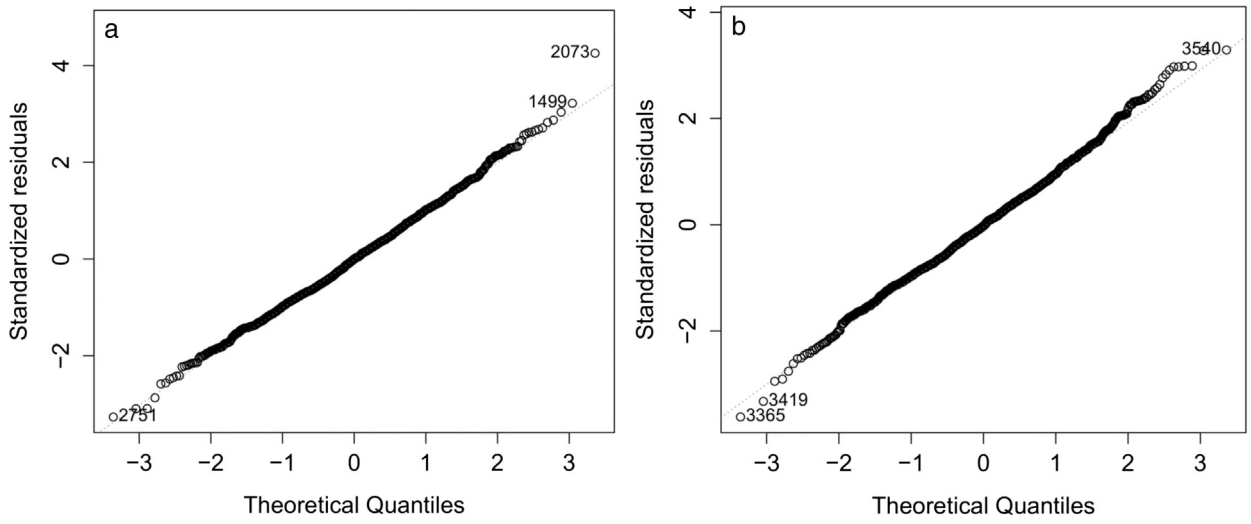

Fig. A.3. Normal Q–Q plots of OLS models with spatial filtering a. Mixed-conifer forests b. Red fir forests.

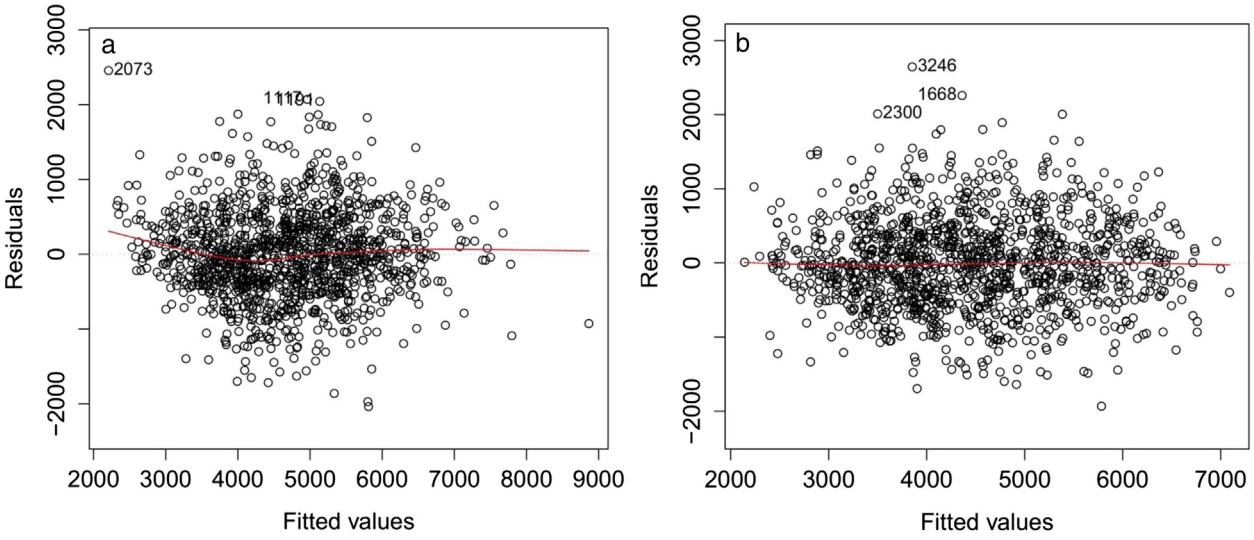

Fig. A.4. Scatterplots of residuals and fitted values of OLS model with spatial filtering a. Mixed-conifer forests b. Red fir forests.

References

Allen, C.D., Macalady, A.K., Chenchouni, H., Bachelet, D., McDowell, N., Vennetier, M., ... Hogg, E.H. (2010). A global overview of drought and heat-induced tree mortality reveals emerging climate change risks for forests. *Forest Ecology and Management*, *259*, 660–684.

Arnold, J.D., Brewer, S., & Dennison, P. (2014). Modeling climate-fire connections within the Great Basin and Upper Colorado River Basin, western United States. *Fire Ecology*, *10*, 64–75.

Batllori, E., Ackerly, D.D., & Moritz, M.A. (2015). A minimal model of fire-vegetation feedbacks and disturbance stochasticity generates alternative stable states in grassland–shrubland–woodland systems. *Environmental Research Letters*, *10*, 034018.

Bivand, R., Anselin, L., Berke, O., Bernat, A., Carvalho, M., Chun, Y., ... Lewin-Koh, N. (2011). spdep: Spatial dependence: Weighting schemes, statistics and models. *R package version 0.5-31* (URL http://CRAN.R-project.org/package=spdep).

Bond-Lamberty, B., Rocha, A.V., Calvin, K., Holmes, B., Wang, C., & Goulden, M.L. (2014). Disturbance legacies and climate jointly drive tree growth and mortality in an intensively studied boreal forest. *Global Change Biology*, *20*, 216–227.

Borcard, D., Legendre, P., Avois-Jacquet, C., & Tuomisto, H. (2004). Dissecting the spatial structure of ecological data at multiple scales. *Ecology*, *85*, 1826–1832.

Boschetti, L., Roy, D.P., Justice, C.O., & Humber, M.L. (2015). MODIS–Landsat fusion for large area 30 m burned area mapping. *Remote Sensing of Environment*, *161*, 27–42.

Broncano, M.J., & Retana, J. (2004). Topography and forest composition affecting the variability in fire severity and postfire regeneration occurring after a large fire in the Mediterranean basin. *International Journal of Wildland Fire*, *13*, 209–216.

Carlson, T.N., Perry, E.M., & Schmugge, T.J. (1990). Remote estimation of soil moisture availability and fractional vegetation cover for agricultural fields. *Agricultural and Forest Meteorology*, *52*, 45–69.

Castro, J., Zamora, R., Hódar, J.A., & Gómez, J.M. (2002). Use of shrubs as nurse plants: A new technique for reforestation in Mediterranean mountains. *Restoration Ecology*, *10*, 297–305.

Castro, J., Zamora, R., Hódar, J.A., Gómez, J.M., & Gómez-Aparicio, L. (2004). Benefits of using shrubs as nurse plants for reforestation in Mediterranean mountains: A 4-year study. *Restoration Ecology*, *12*, 352–358.

Chappell, C.B., & Agee, J.K. (1996). Fire severity and tree seedling establishment in Abies magnifica forests, southern CCascades, Oregon. *Ecological Applications*, 628–640.

Chen, X., Vogelmann, J.E., Rollins, M., Ohlen, D., Key, C.H., Yang, L., ... Shi, H. (2011). Detecting postfire burn severity and vegetation recovery using multitemporal remote sensing spectral indices and field-collected composite burn index data in a ponderosa pine forest. *International Journal of Remote Sensing*, *32*, 7905–7927.

Chu, T., & Guo, X. (2013). Remote sensing techniques in monitoring postfire effects and patterns of forest recovery in boreal forest regions: A review. *Remote Sensing*, *6*, 470–520.

Clemente, R.H., Cerrillo, R.M.N., & Gitas, I.Z. (2009). Monitoring post-fire regeneration in Mediterranean ecosystems by employing multitemporal satellite imagery. *International Journal of Wildland Fire*, *18*, 648–658.

Collins, B., & Roller, G. (2013). Early forest dynamics in stand-replacing fire patches in the northern Sierra Nevada, California, USA. *Landscape Ecology*, *28*, 1801–1813.

Collins, B.M., Kelly, M., Van Wagtendonk, J.W., & Stephens, S.L. (2007). Spatial patterns of large natural fires in Sierra Nevada wilderness areas. *Landscape Ecology*, *22*, 545–557.

Collins, B.M., Miller, J.D., Thode, A.E., Kelly, M., Van Wagtendonk, J.W., & Stephens, S.L. (2009). Interactions among wildland fires in a long-established Sierra Nevada natural fire area. *Ecosystems*, *12*, 114–128.

Conard, S.G., Jaramillo, A.E., & Cromack, K., Jr. (1985). The role of the genus *Ceanofhus* in western forest ecosystems. *Geneal Technical Report*. Portland, Oregon: U.S. Department of Agriculture, Forest Service, Pacific Northwest Research Station PNW-GTR-182.

Cook, R.D. (2009). *Regression graphics: ideas for studying regressions through graphics*, *482*, John Wiley & Sons.

Craney, T.A., & Surles, J.G. (2002). Model-dependent variance inflation factor cutoff values. *Quality Engineering*, *14*, 391–403.

Crotteau, J.S., Morgan Varner, J., III, & Ritchie, M.W. (2013). Postfire regeneration across a fire severity gradient in the southern Cascades. *Forest Ecology and Management*, *287*, 103–112.

Csiszar, I., Schroeder, W., Giglio, L., Ellicott, E., Vadrevu, K.P., Justice, C.O., & Wind, B. (2014). Active fires from the Suomi NPP Visible Infrared Imaging Radiometer Suite: Product status and first evaluation results. *Journal of Geophysical Research: Atmospheres*, *119*, 803–881.

Dale, V.H., Joyce, L.A., McNulty, S., Neilson, R.P., Ayres, M.P., Flannigan, M.D., ... Wotton, B.M. (2001). Climate change and forest disturbances. *BioScience*, *51*, 723–734.

Daly, C., Neilson, R.P., & Phillips, D.L. (1994). A statistical–topographic model for mapping climatological precipitation over mountainous terrain. *Journal of Applied Meteorology*, *33*, 140–158.

D'Antonio, C.M., & Vitousek, P.M. (1992). Biological invasions by exotic grasses, the grass/fire cycle, and global change. *Annual Review of Ecology and Systematics*, *23*, 63–87.

Daskalakou, E.N., & Thanos, C.A. (1996). Aleppo pine (*Pinus halepensis*) postfire regeneration: The role of canopy and soil seed banks. *International Journal of Wildland Fire*, *6*, 59–66.

De Knegt, H.J., van Langevelde, F. v., Coughenour, M.B., Skidmore, A.K., De Boer, W.F., Heitkönig, I.M.A., ... Prins, H.H.T. (2010). Spatial autocorrelation and the scaling of species-environment relationships. *Ecology*, *91*, 2455–2465.

De Santis, A., & Chuvieco, E. (2007). Burn severity estimation from remotely sensed data: Performance of simulation versus empirical models. *Remote Sensing of Environment*, *108*, 422–435.

De Santis, A., & Chuvieco, E. (2009). GeoCBI: A modified version of the Composite Burn Index for the initial assessment of the short-term burn severity from remotely sensed data. *Remote Sensing of Environment*, *113*, 554–562.

Dennison, P.E., Brewer, S.C., Arnold, J.D., & Moritz, M.A. (2014). Large wildfire trends in the western United States, 1984–2011. *Geophysical Research Letters*, *41*, 2928–2933.

Díaz-Delgado, R., & Pons, X. (2001). Spatial patterns of forest fires in Catalonia (NE of Spain) along the period 1975–1995: Analysis of vegetation recovery after fire. *Forest Ecology and Management*, *147*, 67–74.

Díaz-Delgado, R., Lloret, F., & Pons, X. (2003). Influence of fire severity on plant regeneration by means of remote sensing imagery. *International Journal of Remote Sensing*, *24*, 1751–1763.

Diniz-Filho, J.A.F., & Bini, L.M. (2005). Modelling geographical patterns in species richness using eigenvector-based spatial filters. *Global Ecology and Biogeography*, *14*, 177–185.

Donato, D.C., Fontaine, J.B., Campbell, J.L., Robinson, W.D., Kauffman, J.B., & Law, B.E. (2009). Conifer regeneration in stand-replacement portions of a large mixed-severity wildfire in the Klamath–Siskiyou Mountains. *Canadian Journal of Forest Research*, *39*, 823–838.

Dunne, J.A., & Parker, V.T. (1999). Species-mediated soil moisture availability and patchy establishment of *Pseudotsuga menziesii* in chaparral. *Oecologia*, *119*, 36–45.

Epting, J., & Verbyla, D. (2005). Landscape-level interactions of prefire vegetation, burn severity, and postfire vegetation over a 16-year period in interior Alaska. *Canadian Journal of Forest Research*, *35*, 1367–1377.

Feng, Z., Chengquan, H., & Zhiliang, Z. (2015). Use of Vegetation Change Tracker and Support Vector Machine to Map Disturbance Types in Greater Yellowstone Ecosystems in a 1984–2010 Landsat Time Series. *Geoscience and Remote Sensing Letters, IEEE*, *12*(2015), 1650–1654.

Flannigan, M.D., Stocks, B.J., & Wotton, B.M. (2000). Climate change and forest fires. *Science of the Total Environment*, *262*, 221–229.

Fox, J., & Weisberg, S. (2010). *An R companion to applied regression*. Sage.

Gao, F., Masek, J., & Wolfe, R.E. (2009). Automated registration and orthorectification package for Landsat and Landsat-like data processing. *Journal of Applied Remote Sensing*, *3* (033515–033515).

Gitas, I., Mitri, G., Veraverbeke, S., & Polychronaki, A. (2012). Advances in remote sensing of postfire vegetation recovery monitoring–A review. In Fatoyinbo (Ed.), *Remote Sensing of Biomass–Principles and Applications*. InTech (Available at http://www.intechopen.com/books/remote-sensing-of-biomass-principles-andapplications/advances-in-remote-sensing-of-postfire monitoring-a-review [Verified 20 June 2013]).

Goforth, B.R., & Minnich, R.A. (2008). Densification, stand-replacement wildfire, and extirpation of mixed conifer forest in Cuyamaca Rancho State Park, southern California. *Forest Ecology and Management*, *256*, 36–45.

Gómez-Aparicio, L., Zamora, R., Gómez, J.M., Hódar, J.A., Castro, J., & Baraza, E. (2004). Applying plant facilitation to forest restoration: A meta-analysis of the use of shrubs as nurse plants. *Ecological Applications*, *14*, 1128–1138.

Greenberg, J.A., Dobrowski, S.Z., & Vanderbilt, V.C. (2009). Limitations on maximum tree density using hyperspatial remote sensing and environmental gradient analysis. *Remote Sensing of Environment*, *113*, 94–101.

Griffith, D.A. (2000). A linear regression solution to the spatial autocorrelation problem. *Journal of Geographical Systems*, *2*, 141–156.

Griffith, D.A. (2003). *Spatial Autocorrelation and Spatial Filtering: Gaining Understanding Through Theory and Scientific Visualization*. Austin, TX: Springer Science & Business Media.

Griffith, D.A., & Peres-Neto, P.R. (2006). Spatial modeling in ecology: The flexibility of eigenfunction spatial analyses. *Ecology*, *87*, 2603–2613.

Henry, M.C., & Hope, A.S. (1998). Monitoring post-burn recovery of chaparral vegetation in southern California using multi-temporal satellite data. *International Journal of Remote Sensing*, *19*, 3097–3107.

Hope, A., Tague, C., & Clark, R. (2007). Characterizing post-fire vegetation recovery of California chaparral using TM/ETM+ time-series data. *International Journal of Remote Sensing*, *28*, 1339–1354.

Huang, C., Goward, S.N., Masek, J.G., Thomas, N., Zhu, Z., & Vogelmann, J.E. (2010a). An automated approach for reconstructing recent forest disturbance history using dense Landsat time series stacks. *Remote Sensing of Environment*, *114*, 183–198.

Huang, C., Thomas, N., Goward, S.N., Masek, J.G., Zhu, Z., Townshend, J.R.G., & Vogelmann, J.E. (2010b). Automated masking of cloud and cloud shadow for forest change analysis using Landsat images. *International Journal of Remote Sensing*, *31*, 5449–5464.

Huang, C., Goward, S.N., Masek, J.G., Gao, F., Vermote, E.F., Thomas, N., ... Eidenshink, J.C. (2009). Development of time series stacks of Landsat images for reconstructing forest disturbance history. *International Journal of Digital Earth*, *2*, 195–218.

Huesca, M., Merino-de-Miguel, S., González-Alonso, F., Martínez, S., Miguel Cuevas, J., & Calle, A. (2013). Using AHS hyper-spectral images to study forest vegetation recovery after a fire. *International Journal of Remote Sensing*, *34*, 4025–4048.

Ireland, G., & Petropoulos, G.P. (2015). Exploring the relationships between postfire vegetation regeneration dynamics, topography and burn severity: A case study from the montane cordillera ecozones of western Canada. *Applied Geography*, *56*, 232–248.

Kane, V.R., Cansler, C.A., Povak, N.A., Kane, J.T., McGaughey, R.J., Lutz, J.A., et al. (2015b). Mixed severity fire effects within the Rim fire: Relative importance of local climate, fire weather, topography, and forest structure. *Forest Ecology and Management*, *358*, 62–79.

Kane, V.R., Lutz, J.A., Alina Cansler, C., Povak, N.A., Churchill, D.J., Smith, D.F., ... North, M.P. (2015a). Water balance and topography predict fire and forest structure patterns. *Forest Ecology and Management*, *338*, 1–13.

Kane, V.R., Lutz, J.A., Roberts, S.L., Smith, D.F., McGaughey, R.J., Povak, N.A., & Brooks, M.L. (2013). Landscape-scale effects of fire severity on mixed-conifer and red fir forest structure in Yosemite National Park. *Forest Ecology and Management*, *287*, 17–31.

Kane, V.R., North, M.P., Lutz, J.A., Churchill, D.J., Roberts, S.L., Smith, D.F., ... Brooks, M.L. (2014). Assessing fire effects on forest spatial structure using a fusion of Landsat and airborne LiDAR data in Yosemite National Park. *Remote Sensing of Environment*, *151*, 89–101.

Kauffman, J.B., & Martin, R.E. (1990). Sprouting shrub response to different seasons and fuel consumption levels of prescribed fire in sierra Nevada mixed conifer ecosystems. *Forest Science*, *36*, 748–764.

Kauffman, J.B., & Martin, R.E. (1991). Factors influencing the scarification and germination of three montane Sierra Nevada shrubs. *Northwest Science*, *65*, 180–187.

Kotrlik, J., & Higgins, C. (2001). Organizational research: Determining appropriate sample size in survey research. *Information Technology, Learning, and Performance Journal*, *19*, 43–50.

Kuhn, M. (2015). Caret: Classification and regression training. *Astrophysics Source Code Library*, *1*. (pp. 05003).

Laacke, R.J., & Tappeiner, J.C. (1996). Red fir ecology and management. Available at http://pubs.usgs.gov/dds/dds-43/VOL_III/VIII_C10.PDF (Verified 20 June 2013)

Lee, R.J., & Chow, T.E. (2015). Post-wildfire assessment of vegetation regeneration in Bastrop, Texas, using Landsat imagery. *GIScience & Remote Sensing*, 1–18.

Lenihan, J.M., Bachelet, D., Neilson, R.P., & Drapek, R. (2008). Response of vegetation distribution, ecosystem productivity, and fire to climate change scenarios for California. *Climatic Change*, *87*, 215–230.

Lentile, L.B., Holden, Z.A., Smith, A.M.S., Falkowski, M.J., Hudak, A.T., Morgan, P., ... Benson, N.C. (2006). Remote sensing techniques to assess active fire characteristics and post-fire effects. *International Journal of Wildland Fire*, *15*, 319–345.

Lichstein, J.W., Simons, T.R., Shriner, S.A., & Franzreb, K.E. (2002). Spatial autocorrelation and autoregressive models in ecology. *Ecological Monographs*, *72*, 445–463.

Lydersen, J., & North, M. (2012). Topographic variation in structure of mixed-conifer forests under an active-fire regime. *Ecosystems*, *15*, 1134–1146.

Mantgem, P.J. v., Stephenson, N.L., & Keeley, J.E. (2006). Forest reproduction along a climatic gradient in the Sierra Nevada, *California*. *Forest Ecology and Management*, *225*, 391–399.

Meng, R., Dennison, P.E., D'Antonio, C.M., & Moritz, M.A. (2014). Remote sensing analysis of vegetation recovery following short-interval fires in Southern California shrublands. *PloS One*, *9*, e110637.

Miller, C., & Urban, D.L. (1999a). A model of surface fire, climate and forest pattern in the Sierra Nevada, California. *Ecological Modelling*, *114*, 113–135.

Miller, C., & Urban, D.L. (1999b). Forest pattern, fire, and climatic change in the Sierra Nevada. *Ecosystems*, *2*, 76–87.

Miller, J.A., & Hanham, R.Q. (2011). Spatial nonstationarity and the scale of species–environment relationships in the Mojave Desert, California, USA. *International Journal of Geographical Information Science*, *25*, 423–438.

Miller, J.D., & Thode, A.E. (2007). Quantifying burn severity in a heterogeneous landscape with a relative version of the delta Normalized Burn Ratio (dNBR). *Remote Sensing of Environment*, *109*, 66–80.

Miller, J.D., Knapp, E.E., Key, C.H., Skinner, C.N., Isbell, C.J., Creasy, R.M., & Sherlock, J.W. (2009a). Calibration and validation of the relative differenced Normalized Burn Ratio (RdNBR) to three measures of fire severity in the Sierra Nevada and Klamath Mountains, California, USA. *Remote Sensing of Environment*, *113*, 645–656.

Miller, J.D., Safford, H.D., Crimmins, M., & Thode, A.E. (2009b). Quantitative evidence for increasing forest fire severity in the Sierra Nevada and southern Cascade Mountains, California and Nevada, USA. *Ecosystems*, *12*, 16–32.
Minore, D., & Laacke, R.J. (1992). Natural regeneration. In S.D. Tesch, S.D. Hobbs, P.W. Owston, R.E. Stewart, J.C. TappeinerII, & G.E. Wells (Eds.), *Forest Research Laboratory* (pp. 258–283). Corvallis, Oregon: Oregon State University.
Mitchell, M., & Yuan, F. (2010). Assessing forest fire and vegetation recovery in the black hills, South Dakota. *GIScience and Remote Sensing*, *47*, 276–299.
Mitri, G.H., & Gitas, I.Z. (2013). Mapping postfire forest regeneration and vegetation recovery using a combination of very high spatial resolution and hyperspectral satellite imagery. *International Journal of Applied Earth Observation and Geoinformation*, *20*, 60–66.
Moran, P.A.P. (1950). Notes on continuous stochastic phenomena. *Biometrika*, *37*, 17–23.
Moritz, M.A., Parisien, M. -A., Batllori, E., Krawchuk, M.A., Van Dorn, J., Ganz, D.J., & Hayhoe, K. (2012). Climate change and disruptions to global fire activity. *Ecosphere*, *3* (art49).
Nagel, T.A., & Taylor, A.H. (2005). Fire and persistence of montane chaparral in mixed conifer forest landscapes in the northern Sierra Nevada, Lake Tahoe Basin, California, USA. *The Journal of the Torrey Botanical Society*, *132*, 442–457.
O'Brien, R.M. (2007). A caution regarding rules of thumb for variance inflation factors. *Quality and Quantity*, *41*, 673–690.
Parker, I., & Matyas, W. (1979). *CALVEG: a classification of Californian vegetation.* Albany, California: U.S. Department of Agriculture, Forest Service, Pacific Southwest Region Station.
Parks, S.A., Dillon, G.K., & Miller, C. (2014). A new metric for quantifying burn severity: the Relativized Burn Ratio. *Remote Sensing*, *6*, 1827–1844.
Polychronaki, A., Gitas, I.Z., & Minchella, A. (2013). Monitoring post-fire vegetation recovery in the Mediterranean using SPOT and ERS imagery. *International Journal of Wildland Fire*, *23*, 631–642.
Riaño, D., Chuvieco, E., Ustin, S., Zomer, R., Dennison, P., Roberts, D., & Salas, J. (2002). Assessment of vegetation regeneration after fire through multitemporal analysis of AVIRIS images in the Santa Monica Mountains. *Remote Sensing of Environment*, *79*, 60–71.
Rodrigues, M., de la Riva, J., & Fotheringham, S. (2014). Modeling the spatial variation of the explanatory factors of human-caused wildfires in Spain using geographically weighted logistic regression. *Applied Geography*, *48*, 52–63.
Rogers, B.M., Neilson, R.P., Drapek, R., Lenihan, J.M., Wells, J.R., Bachelet, D., & Law, B.E. (2011). Impacts of climate change on fire regimes and carbon stocks of the U.S. Pacific Northwest. *Journal of Geophysical Research, G: Biogeosciences*, *116*, G03037.
Rouse, J.J.W., Haas, R.H., Schell, J.A., & Deering, D.W. (1974). Monitoring vegetation systems in the Great Plains with ERTS. *NASA special publication*, *351*, 309.
Roy, D.P., Boschetti, L., & Trigg, S.N. (2006). Remote sensing of fire severity: assessing the performance of the normalized burn ratio. *IEEE Geoscience and Remote Sensing Letters*, *3*, 112–116.
Russell, W.H., McBride, J.R., & Rowntree, R. (1998). Revegetation after four stand-replacing fires in the Lake Tahoe basin. *Madrono*, *45*, 40–46.
Sánchez-Gómez, D., Valladares, F., & Zavala, M.A. (2006). Performance of seedlings of Mediterranean woody species under experimental gradients of irradiance and water availability: Trade-offs and evidence for niche differentiation. *New Phytologist*, *170*, 795–806.
Scholl, A.E., & Taylor, A.H. (2006). Regeneration patterns in old-growth red fir–western white pine forests in the northern Sierra Nevada, Lake Tahoe, USA. *Forest Ecology and Management*, *235*, 143–154.
Schwartz, M.W., Butt, N., Dolanc, C.R., Holguin, A., Moritz, M.A., North, M.P., ... van Mantgem, P.J. (2015). Increasing elevation of fire in the Sierra Nevada and implications for forest change. *Ecosphere*, *6* (art121).
Shatford, J.P.A., Hibbs, D.E., & Puettmann, K.J. (2007). Conifer regeneration after forest fire in the Klamath–Siskiyous: How much, how soon? *Journal of Forestry*, *105*, 139–146.
Solans Vila, J.P., & Barbosa, P. (2010). Postfire vegetation regrowth detection in the Deiva Marina region (Liguria-Italy) using Landsat TM and ETM+ data. *Ecological Modelling*, *221*, 75–84.
Storer, T.I., & Usinger, R.L. (1963). *Sierra Nevada Natural History: An illustrated Handbook.* Berkeley, California: University of California Press.
Sugihara, N.G., Wagtendonk, J.W.V., Shaffer, K.E., Fites-Kaufman, J., & Andrea, E.T. (2006). *Fire in California's ecosystems*. Berkeley, CA: University of California Press.
Swetnam, T.W., Baisan, C.H., Morino, K., & Caprio, A.C. (1998). Fire history along elevational transects in the Sierra Nevada, California. *Final report to the Sierra Nevada global change research program*. University of Arizona, Laboratory of Tree-ring Research.
Tanase, M., de la Riva, J., Santoro, M., Pérez-Cabello, F., & Kasischke, E. (2011). Sensitivity of SAR data to post-fire forest regrowth in Mediterranean and boreal forests. *Remote Sensing of Environment*, *115*, 2075–2085.
Tanase, M., Santoro, M., de La Riva, J., Pérez-Cabello, F., & Le Toan, T. (2010a). Sensitivity of X-, C-, and L-band SAR backscatter to burn severity in Mediterranean pine forests. *IEEE Transactions on Geoscience and Remote Sensing*, *48*, 3663–3675.
Tanase, M.A., Santoro, M., Wegmüller, U., de la Riva, J., & Pérez-Cabello, F. (2010b). Properties of X-, C-and L-band repeat-pass interferometric SAR coherence in Mediterranean pine forests affected by fires. *Remote Sensing of Environment*, *114*, 2182–2194.
Tappeiner, J.C., Newton, M., McDonald, P.M., & Harrington, T.B. (1992). Ecology of hardwoods, shrubs, and herbaceous vegetation: effects on conifer regeneration. Reforestation practices in southwestern Oregon and northern California. *Forest Research Laboratory* (pp. 136–164). Corvallis, Oregon: Oregon State University.
Taylor, A.H., & Halpern, C.B. (1991). The structure and dynamics of abies magnifica forests in the southern Cascade Range, USA. *Journal of Vegetation Science*, *2*, 189–200.
Taylor, A.H., & Skinner, C.N. (1998). Fire history and landscape dynamics in a late-successional reserve, Klamath Mountains, California, USA. *Forest Ecology and Management*, *111*, 285–301.
Thayn, J.B., & Simanis, J.M. (2013). Accounting for spatial autocorrelation in linear regression models using spatial filtering with eigenvectors. *Annals of the Association of American Geographers*, *103*, 47–66.
Thomas, N.E., Huang, C., Goward, S.N., Powell, S., Rishmawi, K., Schleeweis, K., & Hinds, A. (2011). Validation of North American Forest disturbance dynamics derived from Landsat time series stacks. *Remote Sensing of Environment*, *115*, 19–32.
Thonicke, K., Venevsky, S., Sitch, S., & Cramer, W. (2001). The role of fire disturbance for global vegetation dynamics: Coupling fire into a dynamic global vegetation model. *Global Ecology and Biogeography*, *10*, 661–677.
Thornton, P.E., Law, B.E., Gholz, H.L., Clark, K.L., Falge, E., Ellsworth, D.S., ... Sparks, J.P. (2002). Modeling and measuring the effects of disturbance history and climate on carbon and water budgets in evergreen needleleaf forests. *Agricultural and Forest Meteorology*, *113*, 185–222.
Veraverbeke, S., Gitas, I., Katagis, T., Polychronaki, A., Somers, B., & Goossens, R. (2012). Assessing post-fire vegetation recovery using red–near infrared vegetation indices: Accounting for background and vegetation variability. *ISPRS Journal of Photogrammetry and Remote Sensing*, *68*, 28–39.
Viedma, O., Meliá, J., Segarra, D., & García-Haro, J. (1997). Modeling rates of ecosystem recovery after fires by using landsat TM data. *Remote Sensing of Environment*, *61*, 383–398.
Wagtendonk, J.W. v., & Fites-Kaufman, J. (2006). Sierra Nevada bioregion. *Fire in California's ecosystems* (pp. 264–294). Berkeley, California, USA: University of California Press.
Wang, Y., Kockelman, K.M., & Wang, X. (2013). Understanding spatial filtering for analysis of land use-transport data. *Journal of Transport Geography*, *31*, 123–131.
Westerling, A.L., Hidalgo, H.G., Cayan, D.R., & Swetnam, T.W. (2006). Warming and earlier spring increase western U.S. forest wildfire activity. *Science*, *313*, 940–943.
White, J.D., Ryan, K.C., Key, C.C., & Running, S.W. (1996). Remote sensing of forest fire severity and vegetation recovery. *International Journal of Wildland Fire*, *6*, 125–136.
Wittenberg, L., Malkinson, D., Beeri, O., Halutzy, A., & Tesler, N. (2007). Spatial and temporal patterns of vegetation recovery following sequences of forest fires in a Mediterranean landscape, Mt. Carmel Israel. *Catena*, *71*, 76–83.